Article

Genetic and morphological variation analyses of *Glandirana rugosa* with description of a new species (Anura, Ranidae)

TOMOHIKO SHIMADA[1*], MASAFUMI MATSUI[2], MITSUAKI OGATA[3], IKUO MIURA[4], MAI TANGE[1,5], MI-SOOK MIN[6] & KOSHIRO ETO[7]

[1]*Department of Science Education, Aichi University of Education, 1 Hirosawa, Igaya, Kariya, Aichi 448–8542, JAPAN*
[2]*Graduate School of Human and Environmental Studies, Kyoto University, Sakyo, Kyoto 606–8501, JAPAN*
✉ *fumi@zoo.zool.kyoto-u.ac.jp;* ⓞ *https://orcid.org/0000-0003-2032-2528*
[3]*Preservation and Research Center, City of Yokohama, 155-1 Asahi Ward, Yokohama 241-0804, JAPAN*
✉ *zvp06246@nifty.com;* ⓞ *https://orcid.org/0000-0001-5346-9847*
[4]*Amphibian Research Center, Hiroshima University, 1-3-1 Kagamiyama, Higashi-Hiroshima 739-8526, JAPAN*
✉ *imiura@hiroshima-u.ac.jp;* ⓞ *https://orcid.org/0000-0003-3564-2882*
[5]*Takahama High School, 1-6-1 Hongo, Takahama, Aichi 444-1311, JAPAN*
✉ *tanma.755@gmail.com;* ⓞ *https://orcid.org/0000-0003-4767-2958*
[6]*Conservation Genome Resource Bank for Korean Wildlife, Research Institute for Veterinary Science and College of Veterinary Medicine, Seoul National University, 1 Gwanak-ro, Seoul 08826, SOUTH KOREA*
✉ *minbio@yahoo.co.kr;* ⓞ *https://orcid.org/0000-0001-9555-7247*
[7]*Kitakyushu Museum of Natural History & Human History, Higashida 2-4-1, Yahatahigashi, Kitakyushu, Fukuoka 805-0071, JAPAN*
✉ *koshiro.eto@gmail.com;* ⓞ *https://orcid.org/0000-0002-8742-7319*
Corresponding author. ✉ *shimadatom@gmail.com;* ⓞ *https://orcid.org/0000-0002-9666-6186*

Abstract

Glandirana rugosa is known to include several geographic groups differing in sex chromosomes, and has been proven to be paraphyletic in mitochondrial phylogeny with respect to *G. susurra*. By analyzing genetic and morphological variation in a large number of individuals of *Glandirana*, we studied their taxonomic relationships. A mitochondrial DNA phylogeny, with the *G. tientaiensis* as outgroup, revealed two major lineages containing respectively (1) the East group of *G. rugosa*, *G. susurra*, and the Central and Southeast-Kyushu groups of *G. rugosa*; and (2) *G. emeljanovi*, and the North and West groups of *G. rugosa*. In contrast, in a nuclear DNA phylogeny based on SNP data, lineages of (1) *G. susurra* and East group, and (2) the remaining groups of *G. rugosa* and *G. emeljanovi*, were split, indicating a distinct status of the East group among *G. rugosa*. In adult morphology, there were only minor differences between the East group and the remaining groups of *G. rugosa*, but in larvae, the East group had significantly more sparse skin glands than the others. The exact type locality of *G. rugosa* is most probably in western Japan, not including the range of the East group. From these results, we describe the East group as a new species, *G. reliquia*, distinct from the remaining groups of *G. rugosa*. The new species with sexually homomorphic chromosomes is thought to represent a basic stock of Japanese *Glandirana*, which existed far before *G. rugosa* originated.

Key words: eastern Japan, *Glandirana rugosa*, larval ventral glands, mitochondrial DNA phylogeny, nuclear DNA phylogeny

Introduction

The ranid frog, *Glandirana rugosa* (Temminck et Schlegel) is endemic to Japan, occurring on Honshu, Shikoku, Kyushu, and adjacent islands. This species was originally described in Philipp Franz von Siebold's "Fauna Japonica" (Temminck & Schlegel 1838), and although type locality was not specified it would be around Nagasaki in western Kyushu, where Siebold stayed long (Stejneger 1907; Maeda & Matsui 1989; Shimada & Matsui 2021). This frog shows relatively large genetic variation (Nishioka *et al*. 1993), and also geographic variation in the mode of sex determination (Nishioka *et al*. 1994). More recently, when *G. susurra* (Sekiya, Miura, and Ogata) (as *Rugosa susurra*) was described from Sado Island as a distinct species, *G. rugosa* showed paraphyletic relationships in a

mitochondrial DNA (mtDNA) tree (Sekiya *et al.* 2012). Namely, *G. susurra* was the sister species to the Kanto (East-Japan), XY, and neo-ZW races of *G. rugosa* (East, Central, and West-Central groups in Oike et al. [2020]), and ZW and West Japan populations (North and West groups in Oike et al. [2020]) outgrouped them, suggesting the necessity of taxonomic reappraisal (Matsui & Maeda 2018). Additionally, Oike *et al.* (2020) found a distinct mtDNA group in southeast Kyushu (se-K), which Nakamura *et al.* (2022) considered as specifically distinct.

For analyzing intraspecific genetic variation of *G. rugosa*, allozyme electrophoresis (Nishioka *et al.* 1993), mtDNA (Ogata *et al.* 2008; Oike *et al.* 2017, 2020; Sekiya *et al.* 2010), and sex-linked genes (Ogata *et al.* 2008) have hitherto been applied. However, these frog species apparently have experienced evolution in which introgressive hybridization occurred between populations once differentiated (Ogata e*t al.* 2008), and analyses targeting only particular portions of the genome will probably not reflect their true evolutionary history. Therefore, we here utilize MIG-seq, a genome-wide analysis of single-nucleotide polymorphisms (SNPs) (Suyama & Matsuki 2015) to reinvestigate intraspecific genetic structure within *G. rugosa*.

As to morphological variation in *G. rugosa*, there is some knowledge published by Sekiya *et al.* (2012) and Oike *et al.* (2020), but a full picture of total geographic variation has not yet been attained, partly because of insufficient sampling and methods of analysis. We thus employed a large number of adults, as well as larvae, of all genetic groups for more sophisticated morphological analyses.

Materials and methods

Within frogs long called *G. rugosa*, several names were given for each geographic and genetic population (Nishioka *et al.* 1993; Ogata *et al.* 2008; Oike *et al.* 2017, 2020). In this study, we follow the known mtDNA phylogeny and recognize five groups: East (E), North (N), Central (C), and West (W), and Southeastern Kyushu (se-K). Of these, the Central group includes the West-Central group of Oike *et al.* (2020), which is recognized by the mode of sex determination, and the West group includes subgroups named as West-Honshu (Wh), West-Shikoku (Ws), and West-Kyushu (Wk) by Oike *et al.* (2020).

Molecular genetic analyses: We analyzed (1) the mitochondrial 12S rRNA and 16S rRNA genes for clarifying relationships of known species of *Glandirana* and related genera, (2) the mitochondrial cytochrome *b* (cyt *b*) gene for elucidating intra- and inter population relationships using a large number of samples, and (3) MIGseq analysis, an approach to obtain single-nucleotide polymorphism (SNP) data from across the nuclear genome (For names of sampling localities, see the supplementary Table 1 deposited in Figshare [DOI: 10.6084/m9.figshare.20290599]).

MtDNA analyses: We extracted total DNA from ethanol-preserved muscle tissue using standard phenol–chloroform extraction procedure, and conducted amplifications of regions chosen by the polymerase chain reaction (PCR). The PCR primers L1091 and H2317 (Shimada *et al.* 2011) were used for amplification. We retrieved sequence data from GenBank for one individual each of *G. minima* (Ting and T'sai), *G. tientaiensis* (Chang), *G. emeljanovi* (Nikolskii), East group of *G. rugosa*, Central group of *G. rugosa*, North group of *G. rugosa*, and West (Wh) group of *G. rugosa*. Also, we added data by sequencing two West (Ws and Wk) and one se-K groups of *G. rugosa*, and one *G. susurra*. Following Pyron and Wiens (2011), we chose *Sanguirana*, *Abavorana*, *Sylvirana*, and *Hylarana* as hierarchical outgroups, and *Pelophylax nigromaculatus* (Hallowell) as the outermost outgroup. Sequences were aligned by the Clustal W option of Bio Edit 7.2.5.0 and ambiguous parts removed by Gblocks (Castresana 2000). For cyt *b* region, sequences were similarly determined, but the primers used were L14759 by Shimada *et al.* (2011) and newly designed rugosa cytb F1 (5'-TYACCGGCCTATTCCTAGC-3'), rugosa cytb R1 (5'-CCTARKGTGGGDAYAAGAAGGAC-3'), and rugosa cytb R2 (5'-GGGTCTTCRACTGGTTGACC-3'). We did not apply Gblocks because the sequences did not contain any insertion/deletion. All newly obtained sequences were submitted to GenBank (accession numbers LC717564–LC717673).

For both mtDNA datasets, ML analyses were performed using RAxML 7.0.3 software (Stamatakis 2014), and BI analyses were conducted using MrBayes v3.1.2 (Huelsenbeck & Ronquist 2001). The optimum substitution model, selected by Kakusan4 (Tanabe 2011) based on the Akaike information criterion, was GTR+G+I. In Bayesian analysis, we ran 10 million generations, sampled a tree every 100 generations, and discarded the initial one-fourth as burn-in. Node supports were estimated by 1,000 bootstrapping replicates using RaxML, and posterior probabilities (BPP) for each branch in the Bayesian tree. We regarded tree topologies with bootstrap values (BS) $\geq$ 70% as sufficiently supported (Hillis & Bull 1993). For the BI analysis, we considered BPP $\geq$ 0.95 as significant support (Leaché & Reeder 2002).

MIG-seq analyses: For MIG-seq analyses, we used 67 *G. rugosa*, four *G. susurra*, and five *G. emeljanovi*. We extracted total DNA following the procedure shown in mtDNA analysis, and sent them to the genetic analyses service of Bioengineering Lab. Co., Ltd. (MGI, DNBSEQ-G400 system). From the raw sequences obtained, we cut primer and adapter sequences from each read using Trimmomatic 0.36 (Bolger *et al.* 2014). We also eliminated the sites with quality score less than 30, and unified the read length by excluding pair reads less than 50 bp and cutting sequences after the 50th site.

The quality-filtered reads were then used as input data for SNP detection with Stacks 1.35 (Catchen *et al.* 2011) following the procedure shown in Matsui *et al.* (2019). The setting of basic parameters are as follows; m = 5, M = 5, and N = 1 in 'ustacks' option, n = 2 in 'cstacks' option, r = 0.70 and p = 10 in 'populations' option. The output formats were PHYLIP and STRUCTURE. From the data in PHYLIP format, we eliminated invariable sites, and estimated the maximum likelihood tree using RAxML-NG (Kozlov *et al.* 2019) with the evolutionary model GTR+G with the corrections of acquisition bias (Leaché *et al.*, 2015). We estimated node supports by 1,000 bootstrapping replications. The obtained data were assessed using STRUCTURE 2.3.4 (Pritchard *et al.* 2000) for number of clusters assumed (K) of 1 to 6 with 1,000,000 MCMC iterations following a burn-in period of 200,000. We estimated Evanno's deltaK value (Evanno *et al.* 2005) by STRUCTURE HARVESTER (Earl & von Holdt 2012). For the data in STRUCTURE format, we also conducted the principal component analysis (PCA) using the package 'adegenet' (Jombart 2008) of R 3.0.3 (R Core Team 2014), and plotted the principal component score of each sample for the first, the second, and the third axes.

Morphological analyses: For morphological analyses, we used adult specimens of 757 *G. rugosa* (447 males and 310 females), 67 *G. susurra* (31 males and 36 females), and 38 *G. emeljanovi* from Korea (19 males and 19 females). Locality names and the number of specimens from each locality are deposited as the supplementary Table 1 in Figshare (DOI: 10.6084/m9.figshare.20290599). Specimens were fixed in 10% formalin and later preserved in 70% ethanol and stored at the Aichi University of Education (AUEZ), Graduate School of Human and Environmental Studies, Kyoto University (KUHE), Kitakyushu Museum of Natural History (KMNH), Kanagawa Prefectural Museum of Natural History (KPM), Institute for Amphibian Biology, Graduate School of Science, Hiroshima University (IABHU), and personal collection of Min Mi-Sook (mms). Sex and maturity of specimens were determined by observation of gonads and secondary male sexual characters, such as presence of nuptial pad on finger, and presence of vocal slits. Females with mature ovaries and/or convoluted oviducts were regarded as adults. Genetic groups in *G. rugosa* were determined by the results of mtDNA analyses and location of collection site.

Adult morphology: For adult specimens we took the following body measurements to the nearest 0.1 mm with dial calipers, and under a binocular dissecting microscope when necessary, following Matsui (1984): (1) snout-vent length (SVL); (2) head length (HL); (3) snout-nostril length (S-NL); (4) nostril-eyelid length (N-EL); (5) snout length (SL); (6) eye length (EL, including eyelid); (7) tympanum-eye length (T-EL); (8) tympanum diameter (TD); (9) head width (HW); (10) internarial distance (IND); (11) intercanthal distance (ICD); (12) interorbital distance (IOD); (13) upper eyelid width (UEW); (14) upper eyelid margin distance (UEMD); (15) forelimb length (FLL); (16) lower arm and hand length (LAL); (17) third finger length (TFL); (18) first finger length (FFL); (19) outer palmar tubercle length (OPTL); (20) inner palmar tubercle length (IPTL); (21) hand length (HAL); (22) forearm width (FAW); (23) hindlimb length (HLL); (24) tibia length (TL); (25) foot length (FL); (26) thigh length (THIGH); (27) first toe length (1TOEL); (28) fourth toe length (FTL); and (29) inner metatarsal tubercle length (IMTL). For a part of the specimens, we also observed the point reached by the tibiotarsal joint when hindlimb is bent forward along the body, degree of development of webbing between two outer toes, and degree of development of outer metatarsal tubercle. For reference, we examined type series of *Rana rugosa* stored in the Rijksmuseum van Natuurlijke Historie, Leiden (RMNH, now Naturalis Biodiversity Center) (Gasso Miracle *et al.* 2007).

Larval skin texture: For larval specimens preserved in formalin, we recorded degree of development of ventral glands, and classified into the following four states (Fig. 1): State A. glands present between throat and abdomen; State B. glands partly absent between throat and abdomen, whole abdomen with glands; State C. glands partly absent between throat and abdomen, center of abdomen without glands; State D. glands nearly absent on ventral side. We compared the numeric proportion of states of ventral glands between each of five groups of *G. rugosa*, and *G. susurra* using the Fisher's exact test (Sokal & Rohlf 1981). To take into account multiple comparisons, the significance level was adjusted using the sequential Bonferroni procedure (Rice 1989).

Statistics: For each sex, we compared SVL by ANOVA with Dunn's multiple comparison tests, while we performed the Kruskal-Wallis test with Tukey-Kramer test for ratio values and detection of the presence or absence

of differences in the frequency distributions. All statistical analyses were performed by R 3.0.3 (R Core Team 2014), and significance level of 5% was used.

For differentiating genetic groups recognized by SNP analyses, we conducted canonical discriminant analysis (CANDISC) using $\log_{10}$-transformed metric values of all the 28 characters. We omitted specimens with missing values.

Acoustic analyses: For the acoustic data, we used frog calls recorded in the field using a digital recorder (SONY ECM-959A) with an external microphone (Audio Technica AT9946CM) at 44.1 kHz/16 bits as uncompressed wave files. We analyzed recordings with Raven Lite 2.0 for Mac OS X on a Macintosh computer. Temporal data were obtained from the oscillogram and frequency information was obtained from the audiospectrograms using Fast Fourier Transformation (1,024-point Hanning window). Definitions of acoustic parameters follow Matsui (1997).
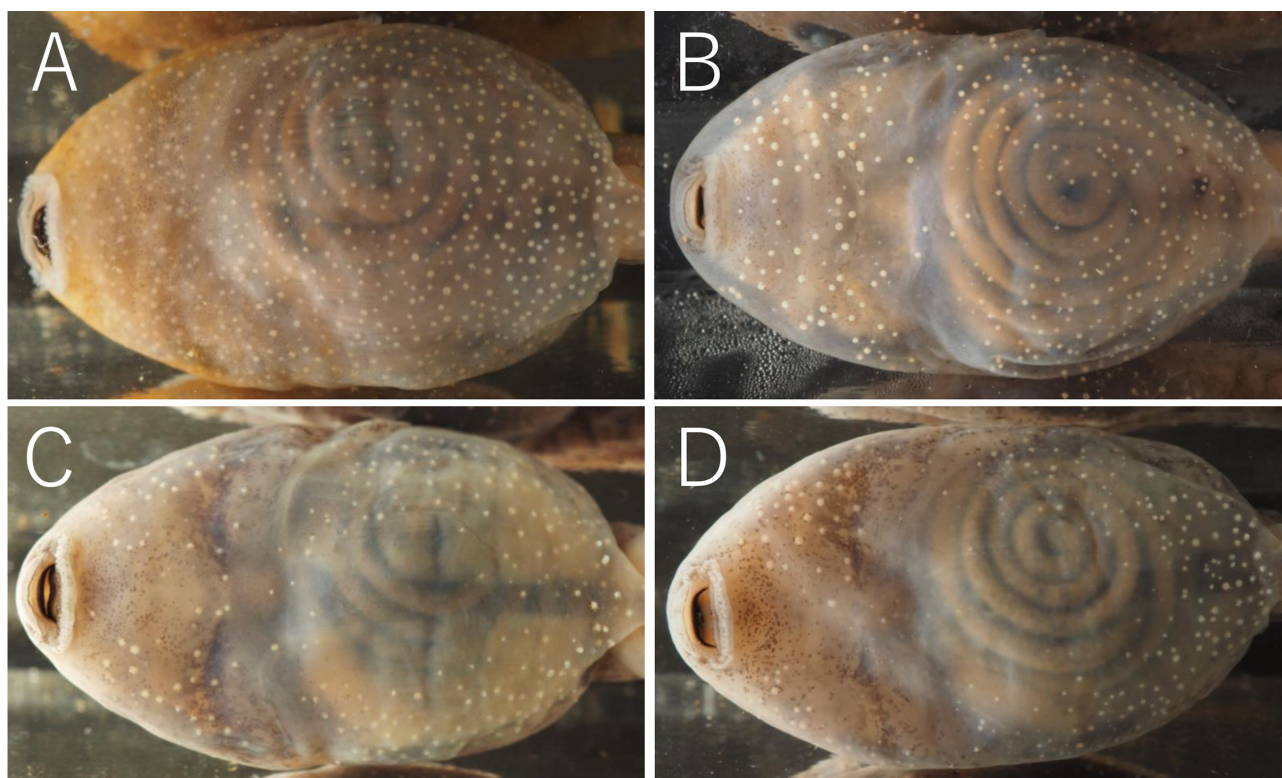

FIGURE 1. Variation in degree of development of larval ventral glands. (A) State A, (B) State B, (C) State C, and (D) State D.

Results

Molecular analysis. MtDNA: We obtained 1,140 bp of 12S and 16S rRNA of mtDNA, of which 357 bp were variable and 206 bp were parsimony informative. The genetic distances among the taxa examined are shown in Table 1 together with those for cyt *b*. Phylogenetic analyses employing RAxML and BI methods yielded nearly identical topologies, and only the RAxML tree is presented in Fig. 2 (left). The genus *Glandirana* formed a monophyletic group with *Sanguirana luzonensis* (Boulenger), in which trichotomous relationships of *S. luzonensis*, *G. minima*, and the remaining *Glandirana* species were observed. Within the last group, *G. tientaiensis* first diverged and the remaining species formed two clades. One of them comprised *G. susurra* and East, Central, and se-K groups of *G. rugosa*, and East and Central groups of *G. rugosa* showed sister group relationship. The other clade consisted of *G. emeljanovi*, North and West groups of *G. rugosa*.

We obtained 918 bp of mitochondrial cyt *b*, of which 405 bp were variable and 342 bp were parsimony informative. Completely identical topologies were obtained between phylogenetic analyses employing RAxML and BI methods, and the RAxML tree is presented in Fig. 2 (right). Phylogenetic relationships were fundamentally identical to those obtained in the analyses of 12S and 16S rRNA of mtDNA. In 16S rRNA, genetic distances varied from 3.1 to 7.0% among the five groups of *G. rugosa*. Distances with *G. susurra* were similar, differing from 4.8 to 6.7% to *G. rugosa* (Table 1).
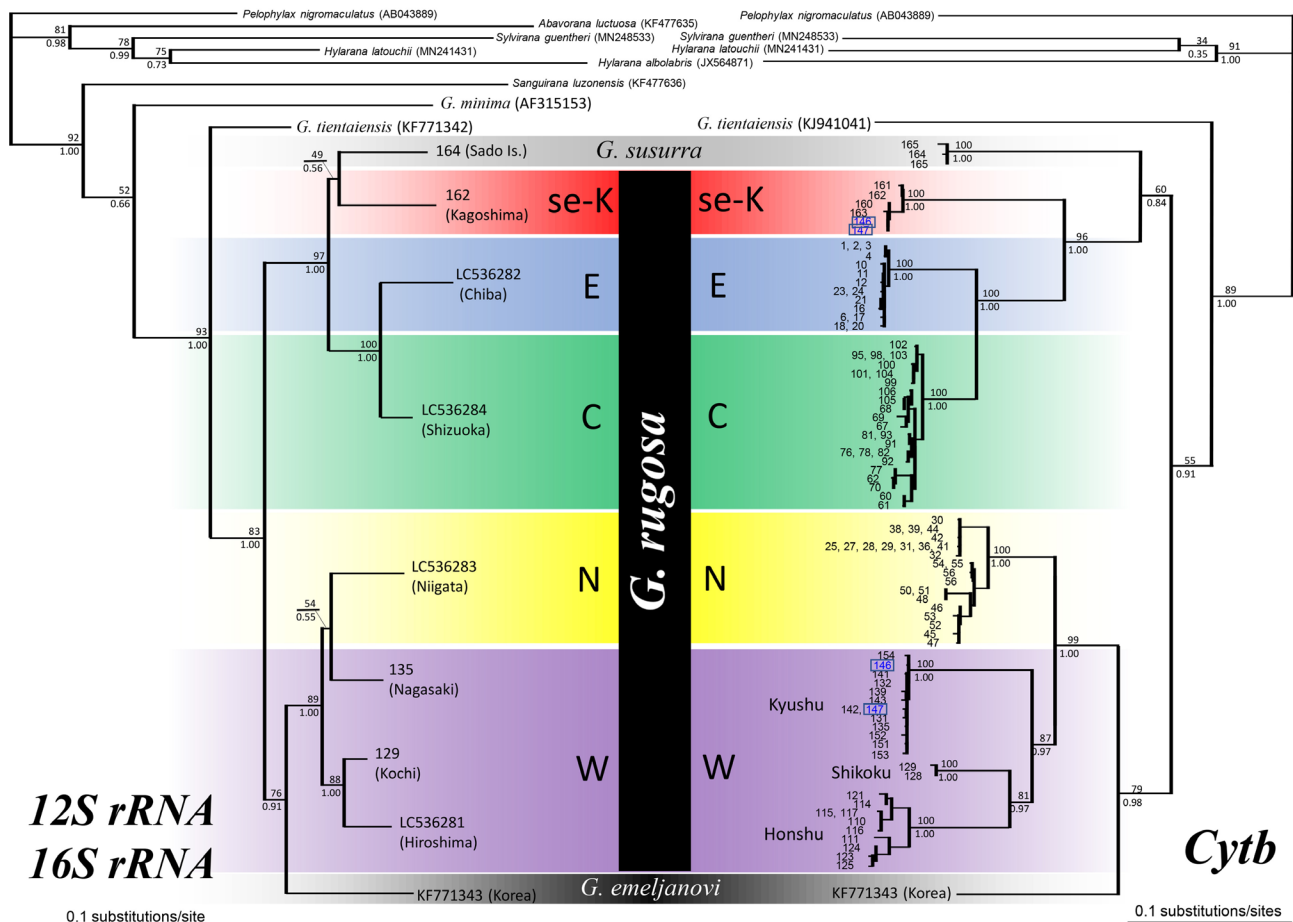
FIGURE 2. RAxML trees based on sequence of mitochondrial 12S and 16S rRNA genes (left) and on sequence of cyt *b* genes (right) for samples of *Glandirana*. Numbers above or below branches represent bootstrap supports for ML inference and Bayesian posterior probability (ML-BS/BPP). Accession numbers are shown for the data obtained from GenBank. Number of each sample corresponds with those shown in the supplementary Table 1 deposited in Figshare (DOI: 10.6084/m9.figshare.20290599). Boxed numbers indicate the locality where we found both of West and se-Kyushu group of *G. rugosa*.

TABLE 1. Uncorrected p-distances (%) among mtDNA lineages of *Glandirana* for 16S rRNA (upper right) and cyt *b* (lower left).

| | G. t. | G. e. | G. s. | E | C | N | W | | | se-K |
							Wh	Ws	Wk	
G. minima	11.5	12.9	14.0	14.0	13.3	12.8	11.5	12.6	13.2	14.8
G. tientaiensis	-	7.9	8.1	8.1	7.3	6.8	6.0	6.9	7.7	7.3
G. emeljanovi	19.9	-	7.1	6.6	7.1	5.2	5.8	5.0	6.6	7.7
G. susurra	19.3	16.3	-	5.6	4.8	6.4	6.7	5.8	5.8	6.2
G. rugosa E	19.0	19.3	15.9	-	3.5	6.4	6.3	6.4	6.2	7.0
G. rugosa C	20.2	18.7	15.2	8.2	-	5.2	5.8	5.8	6.2	5.4
G. rugosa N	18.7	15.9	15.4	18.2	18.1	-	3.2	3.1	3.1	5.6
G. rugosa Wh	19.7	16.9	17.0	17.6	18.4	11.6	-	2.4	3.8	5.8
G. rugosa Ws	19.5	17.4	16.9	17.0	18.0	10.9	10.0	-	4.2	6.2
G. rugosa Wk	20.6	17.1	16.9	17.6	18.9	11.8	12.3	10.7	-	6.8
G. rugosa se-K	22.3	19.2	17.7	14.1	14.0	17.8	17.3	16.8	18.5	-

MIG-seq analyses: After elimination of invariable sites, we obtained 312 SNPs. Unrooted tree obtained from the sequence data largely differed from mtDNA trees (Fig. 3A). Four clusters, (1) East group of *G. rugosa*, (2) *G. susurra*, (3) *G. emeljanovi*, and (4) the remaining groups of *G. rugosa*, were recognized. Since no appropriate outgroup was available and the tree was unrooted, the order of divergence could be estimated limitedly. However, from the shape of tree and branch lengths, we assume that the East group of *G. rugosa* and *G. susurra* are close to each other, and the remaining *G. rugosa* are relatively close to *G. emeljanovi*.

Also in the result of principal component analysis (PCA), the above four clusters, (1) East group of *G. rugosa*, (2) *G. susurra*, (3) *G. emeljanovi*, and (4) *G. rugosa* other than East group, were clearly separated (Fig. 3B, C). The proportion of contribution for the first to fifth axis was 11.4%, 8.5%, 6.8%, 5.3%, and 3.4%, respectively.

Among 78 individuals of *Glandirana* from mtDNA clades, 397 genomic SNP loci were scored and subjected to estimation of genetic structure. As a result, Evanno's deltaK was highest at K = 2. Clustering at K = 2 was discordant with separation of major mtDNA clades, and resulted in separation of East group + *G. susurra* + *G. emeljanovi*, and the remaining groups of *G. rugosa* (Fig. 3D).
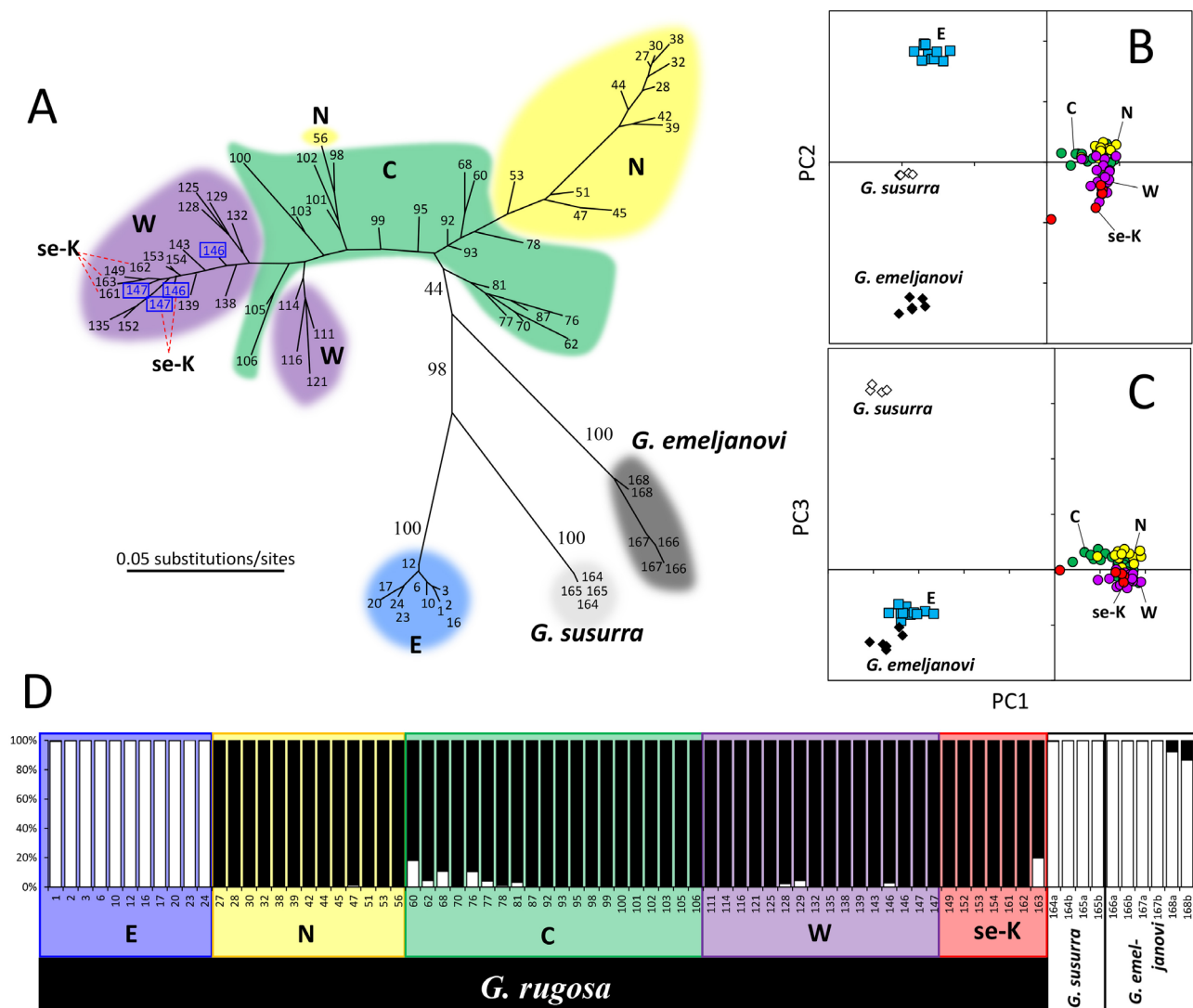

FIGURE 3. Results of MIG-seq (Multiplexed ISSR genotyping by sequencing), showing unique position of East group. (A) A RAxML tree based on variable sites picked up from SNPs data. Numbers above branches represent bootstrap supports for ML inference. Number of each sample corresponds with those shown in the supplementary Table 1 deposited in Figshare (DOI: 10.6084/m9.figshare.20290599). Boxed numbers indicate the locality where we found both of West and se-Kyushu group of *G. rugosa*. (B, C) Plot of first against second (B) and third (C) principal scores of 397 alleles derived from SNPs data. Squares: East group of *G. rugosa*; Open diamonds: *G. susurra*; Closed diamonds: *G. emeljanovi*; Circles: Central, North, West, and se-Kyushu groups of *G. rugosa*. (D) Genetic structure in each individual of mitochondrial groups of *Glandirana*. Two primary genetic demes (K = 2) identified by the STRUCTURE analysis.

Morphological analysis: Adult body size: In males, *G. rugosa*, except for North group showed a tendency to increase SVL from east to west (Table 2: significantly different in Kruskal-Wallis test: East group < West and se-K groups; Central group < West and se-K groups), but North group was eminently large within east Japanese groups (North group > East, Central, and West groups). *Glandirana susurra* tended to be smaller than the sympatric North group, and *G. emeljanovi* tended to be larger than *G. rugosa* from east Japan other than the North group (East and Central groups < *G. emeljanovi*). In females, there were no significant tendencies except that the Central group tended to be smaller than the others (Central group < North and se-K groups). *Glandirana susurra* was relatively small and significantly smaller than *G. rugosa* including the sympatric North group (*G. susurra* < East, North, and se-K groups), while *G. emeljanovi* had significantly larger SVL than all the others.

Ratios of each character to SVL: In males, the East group of *G. rugosa* had larger relative values in S-NL, TD, and IOD than the se-K group of *G. rugosa* (Table 2). From the North group, males of the East group of *G. rugosa* had larger relative values in S-NL, IOD, UEMD, FLL, LAL, OPTL, HAL, FL, and FTL, from the Central group, they had larger TD, UEMD, FLL, LAL, TFL, OPTL, HAL, HLL, TL, and FL, and from the Western group, they had larger S-NL, TD, FLL, HLL, TL and FL. Males of the East group of *G. rugosa* differed from *G. susurra* in larger relative values to SVL in HL, N-EL, SL, TD, HW, ICD, UEW, UEMD, TFL, FFL, and HAL. From *G. emeljanovi*, males of the East group of *G. rugosa* differed in larger TD, HW, UEMD, FLL, LAL, TFL, FFL, HAL, HLL, and FL, all relative to SVL.

In females, the East group of *G. rugosa* had larger relative values in TD and OPTL than the Central group. From the West group, females of the East group of *G. rugosa* differed by larger relative values in TD. Females of the East group of *G. rugosa* differed from *G. susurra* in larger relative values to SVL in HL, EL, HW, ICD, UEW, UEMD, TFL, FFL, and HAL, but smaller value in IPTL. From *G. emeljanovi*, females of the East group of *G. rugosa* differed in larger TD, UEMD, FLL, LAL, TFL, FFL, HAL, FAW, HLL, FL, and FTL.

CANDISC analysis: We conducted CANDISC analysis for four genetic groups recognized by SNP analyses, the East group of *G. rugosa*, *G. emeljanovi*, *G. susurra*, and the remaining groups of *G. rugosa* (North, Central, West, and se-K). In both sexes, CANDISC analysis revealed that the ranges of *G. susurra* and *G. emeljanovi* tended to be separated from *G. rugosa* that largely overlapped with each other on the first two axes (CAN1–CAN2) (Fig. 4). In males, the eigenvalues of the first (CAN1) and second (CAN2) axes accounted for 1.012 (proportion: 0.514) and 0.749 (proportion: 0.381), respectively. On the first axis, the highest absolute magnitude of the standardized canonical discriminant coefficients was −1.106 of OPTL, followed by HW (0.919), and TD (0.911). On the second axis, SL (−1.702), UEMD (0.979), and OPTL (0.973) were high contributors. In females, the eigenvalues of the first (CAN1) and second (CAN2) axes accounted for 1.467 (proportion: 0.511) and 1.249 (proportion: 0.435), respectively. On the first axis, the highest absolute magnitude of the standardized canonical discriminant coefficients was −1.186 of OPTL, followed by HW (1.071), and IND (0.888). On the second axis, SL (−1.332), TD (1.200), and N-EL (1.013) were high contributors.

Degree of development of ventral glands in larvae: In tadpoles of the East group (n = 67), numeric proportion of state A (glands present between throat and abdomen) was smaller (17.9%) than state B (glands partly absent between throat and abdomen, whole abdomen with glands, 23.9%), state C (glands partly absent between throat and abdomen, center of abdomen without glands, 28.7%), and state D (glands nearly absent on ventral side, 31.3%). In contrast, proportion of state A was much larger than the other states in the other groups (100% in the Central group (n = 79) and the southeastern Kyushu group (n = 12), 96.3% in the North group (n = 160), 93.9% in the West group (n = 49), and 90% in *G. susurra* (n = 20) (Fig. 5). The East group significantly differed (P < 0.01) from each of the other five groups, which did not differ significantly from each other. Thus, tadpoles of the East group can be differentiated from all others nearly completely by the condition of ventral glands.

To summarize, paraphyly of *G. rugosa* with respect to *G. susurra* was recognized in the mtDNA tree, whereas in SNP analyses representative of the nuclear genome, the East group was clearly split from the remaining groups of *G. rugosa*. Compared with genome-wide analyses, analyses using only parts of the mitochondrial genome can easily be biased from some evolutionary events, such as introgression, and sometimes does not reflect true evolutional history of the populations (e. g. Ballard & Whitlock 2004). Thus, results of SNP analyses, which rely on information representative for the full nuclear genome, can be expected to better reflecting the population evolutional history.

The East group of *G. rugosa* showed little trace of hybridization between the geographically adjacent North and Central groups in SNP analyses, and was very clearly distinguishable from them. Although the East group of *G. rugosa* has no unique adult morphology sharply distinguishing all the other groups, it had significantly less

developed ventral glands in larvae. From these genetic and morphological properties, the East group is considered as a species distinct from other groups of *G. rugosa*. Although the exact type locality of *G. rugosa* is unknown, it would be in western Japan, far from the range of the East group.
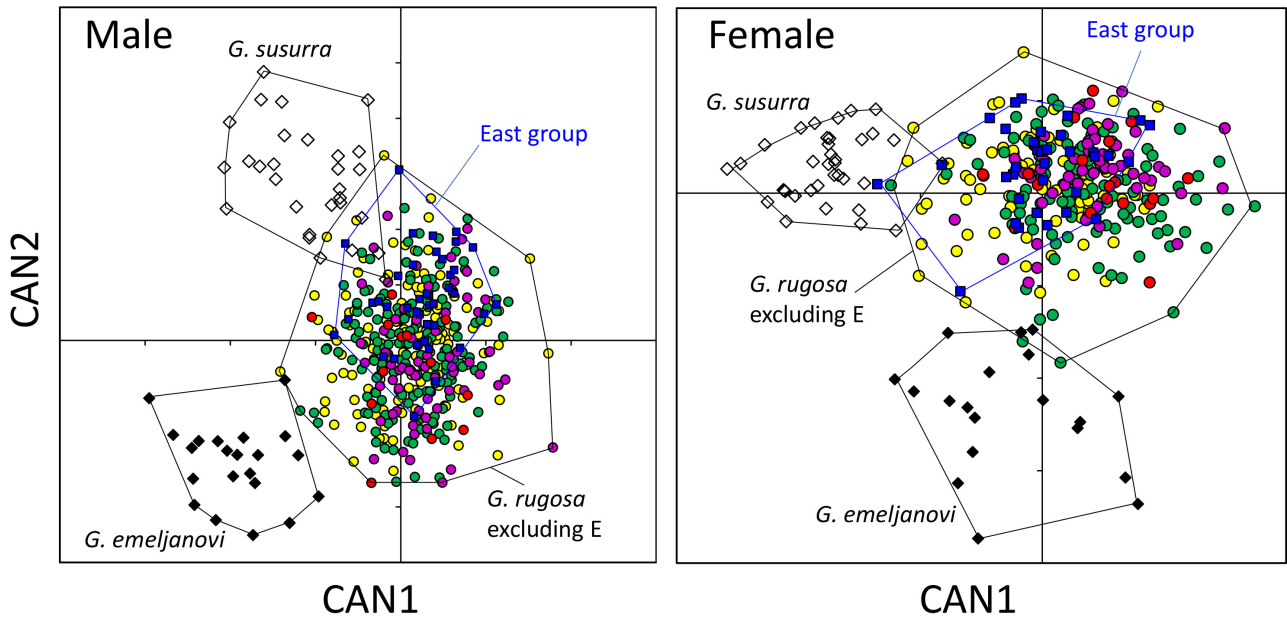

FIGURE 4. Plot of first against second canonical 28 morphological variates from CANDISC for male (left) and female (right) samples of *Glandirana*. Squares: East group of *G. rugosa*; Open diamonds: *G. susurra*; Closed diamonds: *G. emeljanovi*; Circles: Central, North, West, and se-Kyushu groups of *G. rugosa*.
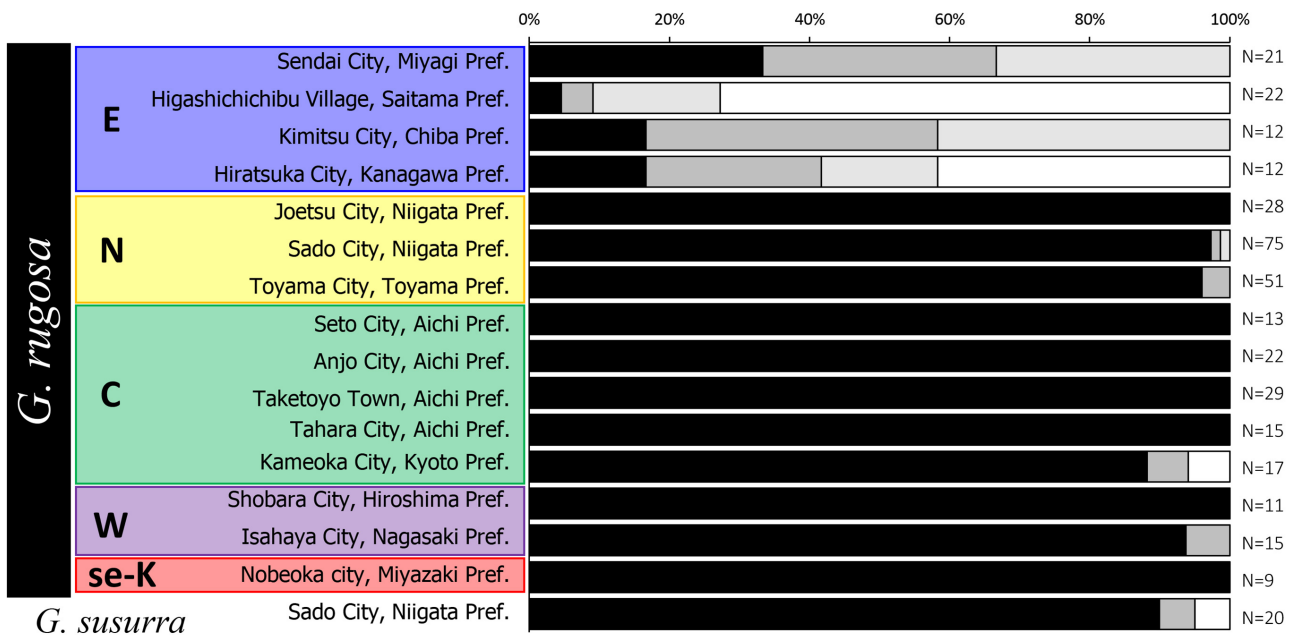

FIGURE 5. Frequencies of four categories of the degree of development of larval ventral glands. Black: state A, dark gray: state B, light gray: state C, and white: state D.

TABLE 2. Measurements in *Glandirana*. SVL (mean ± SD, in mm) and medians of ratios (R) of other characters to SVL, followed by ranges in parentheses. See text for character abbreviations.

males	G. rugosa					G. susurra	G. emeljanovi
	East	North	Central	West	southeast-Kyushu		
n	41	148	179	67	13	31	19
SVL	36.8±1.0	41.3±0.7	37.1±0.49	39.5±0.89	41.2±1.5	38.3±0.7	40.1±2.98
	(28.7–43.0)	(31.3–51.1)	(30.7–51.9)	(32.0–48.3)	(36.0–45.2)	(32.5–43.6)	(31.3–59.1)
rHL	39.8 (37.2–42.9)	39.3 (35.7–44.0)	39.4 (33.9–44.2)	39.7 (36.0–45.0)	40.0 (37.1–41.1)	36.8 (34.5–43.3)	39.5 (36.9–46.1)
rS-NL	8.2 (6.6–9.7)	7.7 (5.5–10.2)	8.0 (6.2–10.2)	7.6 (6.0–9.0)	7.3 (6.2–7.8)	7.8 (6.6–8.6)	7.5 (6.1–9.0)
rN-EL	9.7 (8.1–11.2)	9.5 (7.7–10.9)	9.6 (8.0–12.0)	9.2 (7.9–10.8)	9.2 (8.2–10.0)	9.1 (7.6–10.5)	9.2 (7.7–10.6)
rSL	16.2 (15.0–17.9)	16.0 (14.3–18.2)	16.3 (13.1–18.6)	15.8 (13.9–17.3)	15.6 (15.0–16.6)	15.2 (13.6–16.5)	16.6 (15.3–17.5)
rEL	13.2 (11.3–14.7)	13.2 (10.0–15.6)	13.4 (11.0–16.2)	13.5 (10.8–15.4)	13.1 (12.5–14.0)	13.4 (12.0–15.3)	12.6 (10.4–14.5)
rT-EL	5.2 (3.6–8.2)	4.8 (3.1–6.9)	5.4 (3.6–7.8)	5.0 (3.4–6.7)	4.4 (3.8–5.4)	5.8 (4.2–6.8)	5.4 (3.8–6.6)
rTD	11.1 (9.1–12.6)	10.8 (7.4–13.9)	10.3 (8.0–13.0)	10.0 (7.5–11.5)	9.2 (8.2–10.5)	10.0 (8.7–12.1)	9.1 (8.0–10.4)
rHW	40.2 (36.9–43.0)	39.5 (35.9–43.6)	39.8 (36.4–45.1)	40.3 (35.9–43)	40.0 (37.9–41.8)	36.4 (33.2–41.2)	37.8 (36.1–39.0)
rIND	8.8 (7.4–10.8)	8.9 (6.9–10.6)	9.0 (7.1–12.1)	8.8 (6.9–10.3)	8.3 (7.6–9.8)	8.5 (6.6–11.0)	8.9 (7.7–10.5)
rICD	19.2 (16.5–21.5)	18.5 (16.5–21.1)	19.1 (16.5–22.9)	18.8 (16.7–21.6)	19.0 (18.6–21.8)	18.0 (15.4–20.8)	18.5 (16.3–20.8)
rIOD	8.8 (6.7–10.6)	8.2 (6.4–9.7)	8.6 (6.6–10.9)	8.3 (5.9–11.8)	7.3 (6.8–8.9)	8.6 (7.5–9.8)	8.2 (6.6–9.9)
rUEW	9.9 (7.5–11.5)	9.4 (6.6–12.1)	9.4 (5.4–12.5)	9.9 (7.8–12.0)	9.8 (8.3–11.9)	8.7 (6.4–10.7)	8.9 (7.4–10.8)
rUEMD	29.4 (27.3–32.1)	28.2 (25.5–33.0)	28.6 (25.3–34.2)	29.1 (26.2–32.5)	28.8 (25.7–30.0)	28.0 (26.3–31.0)	27.3 (25.9–28.2)
rFLL	67.9 (62.5–72.5)	65.0 (53.1–75.6)	65.5 (57.4–74.6)	64.7 (56.1–73.2)	66.5 (62.1–73.3)	66.0 (60.0–71.0)	62.3 (56.4–72.7)
rLAL	50.2 (47.4–55.2)	48.5 (40.0–54.7)	48.8 (42.8–55.5)	48.9 (42.4–54.9)	49.7 (46.4–56.5)	48.7 (44.2–52.7)	44.9 (41.7–48.4)
rTFL	17.0 (14.9–18.7)	16.4 (12.0–19.6)	16.3 (12.5–21.0)	16.9 (13.4–20.9)	17.2 (15.3–20.5)	15.2 (13.1–18.5)	14.7 (12.9–17.7)
rFFL	11.2 (8.6–13.7)	10.6 (6.9–13.1)	10.4 (6.9–14.9)	10.7 (7.8–14.2)	11.0 (9.1–12.8)	9.4 (7.7–13.5)	9.0 (6.7–10.7)
rOPTL	4.9 (3.8–6.6)	4.1 (2.6–6.2)	4.2 (2.6–6.1)	4.5 (3.4–7.2)	4.2 (3.3–5.8)	4.9 (3.7–8.2)	4.9 (3.3–5.8)
rIPTL	7.4 (5.0–9.0)	7.1 (4.7–10.2)	7.4 (4.6–10.2)	6.7 (4.0–9.3)	6.3 (5.5–7.6)	8.1 (5.3–10.0)	6.9 (4.9–9.4)
rHAL	28.2 (25.2–31.8)	27.3 (21.7–30.8)	27.2 (23.5–30.3)	27.9 (23.0–31.6)	28.9 (25.6–31.7)	27.0 (24.5–29.7)	26.6 (23.6–29.7)
rFAW	7.9 (6.2–12.2)	8.1 (3.8–10.9)	8.2 (5.2–10.7)	7.9 (5.7–10.7)	8.2 (6.4–9.0)	8.2 (6.4–11.1)	7.4 (5.8–9.6)
rHLL	165.6 (156.5–181.3)	162.1 (141.6–190.0)	159.1 (136.4–176.5)	158.9 (128.9–179.1)	169.9 (152.5–184.6)	166.1 (149.7–177.3)	155.9 (139.5–170.8)
rTL	50.3 (47.5–55.4)	49.1 (42.4–57.9)	48.5 (40.6–56.3)	48.4 (40.1–54.4)	50.8 (48.2–57.1)	50.0 (45.3–54.0)	50.1 (45.4–53.4)
rFL	56.3 (51.3–59.5)	53.4 (45.2–63.1)	52.4 (38.6–58.6)	53.1 (39.0–60.0)	54.2 (52.3–59.9)	54.4 (48.9–58.9)	51.2 (41.3–57.5)
rFTL	10.7 (8.7–12.2)	10.0 (7.5–12.3)	10.1 (5.9–12.1)	10.3 (6.5–15.4)	10.5 (9.3–11.7)	10.3 (8.4–11.5)	10.0 (4.0–13.2)
rIMTL	4.9 (3.7–8.1)	4.7 (3.2–7.7)	5.6 (3.4–8.6)	5.4 (4.1–8.5)	4.9 (4.1–5.2)	4.6 (3.3–6.5)	5.0 (3.6–7.2)

TABLE 2. (Continued)

females	G. rugosa					G. susurra	G. emeljanovi
	East	North	Central	West	southeast-Kyushu		
n	35	86	113	59	18	36	19
SVL	47.9±1.4 (30.5–53.7)	48.8±1.2 (34.4–63.5)	46.4±1.02 (37.3–61.6)	47.2±1.04 (39.2–62.1)	50.5±1.7 (42.5–55.4)	44.9±0.9 (38.0–50.9)	55.4±1.53 (46.9–62.1)
rHL	37.5 (34.9–40.5)	37.7 (34.6–40.6)	37.8 (33.1–41.0)	38.2 (31.1–42.9)	38.7 (35.1–40.6)	35.8 (34.1–45.9)	37.0 (35.4–38.6)
rS-NL	7.2 (5.9–8.8)	7.4 (6.0–9.0)	7.4 (6.0–9.0)	6.9 (5.4–8.3)	6.5 (6.0–8.2)	7.4 (5.7–8.6)	7.1 (5.9–8.2)
rN-EL	9.0 (7.2–10.2)	8.9 (7.4–10.5)	9.1 (7.8–10.8)	8.9 (7.7–11.3)	8.7 (7.6–10.0)	8.5 (7.1–9.5)	8.7 (7.6–10.5)
rSL	15.2 (14.2–17.3)	15.2 (13.5–16.8)	15.2 (13.5–17.3)	15.0 (13.1–17.9)	15.0 (14.3–16.0)	14.7 (13.2–15.8)	15.4 (14.5–16.7)
rEL	12.4 (11.0–14.5)	12.2 (10.1–15.0)	12.3 (10.6–13.9)	12.6 (10.8–16.5)	12.8 (11.3–13.3)	12.9 (11.7–14.6)	11.0 (9.3–12.3)
rT-EL	4.7 (3.3–5.7)	4.8 (3.5–6.0)	4.9 (3.2–6.7)	4.7 (2.9–7.0)	4.5 (3.8–5.7)	5.2 (4.0–6.4)	4.9 (3.3–6)
rTD	9.2 (8.0–10.9)	9.0 (7.9–11.3)	8.7 (7.0–10.3)	8.8 (6.5–10.8)	8.6 (7.2–9.3)	8.8 (7.6–9.8)	7.8 (6.1–9.4)
rHW	39.0 (36.1–41.3)	38.3 (35.6–41.3)	38.8 (34.5–43.2)	39.3 (35.6–46.1)	39.4 (36.2–40.9)	35.5 (33.5–39.8)	37.8 (35.2–40.5)
rIND	8.3 (7.3–9.5)	8.6 (7.0–10.7)	8.6 (6.7–10.4)	8.4 (7.2–10.7)	8.1 (6.9–9.1)	8.0 (6.9–9.2)	8.4 (7.3–10.3)
rICD	18.4 (16.3–20.4)	18.0 (15–20.8)	18.2 (15.2–20.8)	18.3 (15.6–22.5)	18.6 (16.7–20.5)	17.3 (15.1–18.9)	17.9 (16.8–19.2)
rIOD	7.9 (7.0–10.5)	7.7 (6.2–10.4)	8.3 (6.4–10.7)	7.7 (5.4–9.2)	7.0 (5.7–8.5)	8.3 (6.9–9.7)	8.2 (6.8–10.7)
rUEW	9.4 (7.7–10.9)	9.2 (5.7–11.0)	9.0 (6.9–11.6)	9.7 (7.2–12.2)	9.8 (8.8–11.4)	8.5 (7.0–9.7)	8.5 (6.7–11.0)
rUEMD	27.9 (26.1–30.2)	27.1 (24.2–30.8)	27.1 (23.1–30.1)	28.0 (24.7–34.6)	28.0 (25.7–30.3)	26.7 (24.7–28.6)	26.1 (25.4–27.7)
rFLL	63.8 (57.4–71.9)	64.1 (56.4–76.2)	63.9 (56.2–72.4)	63.5 (56.6–71.3)	62.5 (57.9–68.5)	64.1 (59.8–67.5)	59.4 (51.6–68.4)
rLAL	48.8 (44.1–53.5)	47.9 (40.2–53.8)	48.0 (41.8–53.4)	48.0 (40.2–54.5)	47.8 (44.5–52.9)	46.8 (43.1–50.0)	43.1 (39.6–46.7)
rTFL	16.7 (13.3–18.8)	16.4 (12.7–19.2)	16.4 (13.4–19.5)	16.6 (13.5–19.4)	16.8 (15.2–19.1)	15 (13.2–16.7)	14.3 (12.9–15.7)
rFFL	12.1 (10.5–14.3)	11.7 (7.9–14.4)	12.2 (9.4–14.7)	11.9 (9.1–16.4)	12.3 (11.3–13.8)	10.4 (8.2–12.2)	10.8 (8.7–11.3)
rOPTL	4.5 (3.5–5.9)	4.1 (3.0–5.8)	4.0 (2.7–5.5)	4.3 (3.2–7.4)	4.3 (2.9–5.3)	4.9 (2.8–6.8)	4.5 (3.4–5.6)
rIPTL	6.0 (4.4–7.2)	6.2 (3.5–8.6)	5.9 (3.2–8.6)	5.6 (2.5–7.5)	4.8 (4.1–6.2)	7.0 (5.8–9.4)	5.6 (4.6–6.5)
rHAL	27.1 (23.5–30.4)	26.9 (22.7–31.5)	26.9 (23.0–30.3)	27.1 (24.1–30.7)	26.9 (25.1–30.1)	26.1 (23.4–28.6)	24.5 (22.4–27.5)
rFAW	6.9 (5.2–8.2)	6.5 (4.1–9.5)	6.6 (4.9–8.6)	6.7 (5.0–8.7)	7.1 (5.9–8.1)	6.2 (4.2–7.7)	5.9 (4.5–7.2)
rHLL	160.9 (148.4–177.1)	159.2 (136.1–177.8)	157.0 (135.4–176.3)	157.1 (128.9–178.3)	160.8 (146.5–175.6)	160.7 (142.5–172.3)	150.5 (138.5–165.5)
rTL	49.1 (44.8–52.7)	49.2 (41.2–55.1)	48.3 (41.1–53.8)	47.9 (40.0–55.6)	48.3 (44.9–52.3)	48.6 (43.2–52.9)	48.2 (43.9–52.9)
rFL	53.6 (45.6–59.9)	52.5 (45.0–58.4)	52.0 (42.5–61.2)	52.0 (44.5–59.1)	52.7 (47.4–60.2)	53.0 (49.2–58.1)	48.5 (40.4–53.3)
rFTL	10.2 (8.7–13.0)	9.7 (7.7–11.7)	9.7 (7.3–12.6)	9.6 (5.3–12.7)	10.0 (7.9–12.0)	9.8 (8.4–10.9)	8.6 (4.4–10.6)
rIMTL	4.3 (3.1–6.3)	4.2 (2.6–7.5)	4.9 (2.8–9.5)	4.9 (3.3–6.7)	4.5 (3.6–5.9)	4.1 (2.6–6.0)	4.3 (3.1–5.0)

Systematics

***Glandirana reliquia* Shimada, Matsui, Ogata et Miura sp. nov.**
(English name: Proto wrinkled frog)
(Japanese name: Mukashi-Tsuchi-gaeru)
(Fig. 6)
urn:lsid:zoobank.org:act:2A54EE1B-6A05-4B6D-90C6-8384EB080720

Rana rugosa (part): Stejneger 1907, p. 123.
Rana (*Rana*) *rugosa* (part): Nakamura & Uéno 1963, p. 49.
Rana (*Rugosa*) *rugosa* (part): Dubois 1992, p. 322.
Rana rugosa Intermediate subgroup of Eastern group: Nishioka *et al*. 1993, p. 126.
Rana rugosa Kanto form: Ogata *et al*. 2002, p. 186.
Glandirana rugosa (part): Frost *et al*. 2006, p. 368.
Rana rugosa Kanto group: Ogata *et al*. 2008, p. 92.
Rugosa rugosa (part): Fei *et al*. 2010, p. 37.
Rugosa rugosa East Japan group: Sekiya *et al*. 2012, p. 59.
Glandirana rugosa East group: Oike *et al*. 2017, p. 446.
Glandirana rugosa East-J group: Ogata *et al*. 2021, p. 2.

Holotype. KUHE 64088 (former AUEZ 1131), an adult male from Hirata, Kimitsu City, Chiba Prefecture, Japan (35°13' N, 139°59' E, 60 m asl), collected on 23 March 2013 by Tomohiko Shimada and Ai Sakabe.

Paratypes. KUHE 64085–64087 (former AUEZ 0973, 1129–1130) three adult males and KUHE 64089 (former AUEZ 1132), an adult female, data same as the holotype.

Referred specimens. AUEZ 1305, 1309, 1311–1313, Oshu City, Iwate Prefecture; KUHE 21569, 21584, Iwaki City, Fukushima Prefecture; AUEZ 0761–0770, 1168, 2025, 2032, 2033, 2037, 2038, 2047, 2141, 2142, 2324, 2326–2331, 2333–2336, Ichikai Town, Tochigi Prefecture; KUHE 36529–36530, Utsunomiya City, Tochigi Prefecture; KUHE 39765–39767, Kanuma City, Tochigi Prefecture; AUEZ 0379–0381, 0386–0396, 0773, 2368, Higashichichibu Village, Saitama Prefecture; KUHE 28395–28399, 46177, Ichihara City, Chiba Prefecture; AUEZ 0843–0844, Kamogawa City, Chiba Prefecture; AUEZ 0399–0404, KUHE 11254, Akiruno City, Tokyo Metropolis; AUEZ 0782, 0845, 0944–0947, 0949, 0953, Sagamihara City, Kanagawa Prefecture; KUHE 05117, Ueda City, Nagano Prefecture.

Etymology. The specific epithet is from a Latin noun denoting relic, alluding to the facts that the species represents a basic stock of Japanese *Glandirana* existing far before the western *G. rugosa* was derived and leaves a part of its own genome within the heteromorphic sex chromosomes of *G. rugosa* (Miura *et al*. 1998; Miura 2007; Mawaribuchi *et al*. 2016).

Diagnosis. A moderate-sized species of the genus *Glandirana*, with adult SVL 31–54 mm in females and 29–43 mm in males. From *G. rugosa*, this new species is differentiated morphologically in only in several morphometric characters relative to SVL in metamorphs, but is fairly different in development of larval skin glands, and definitely differs from them in nuclear genome characters. It differs from *G. susurra* and *G. emeljanovi*, in ratios of morphometric characters and ventral coloration, from *G. tientaiensis* by less flat dorsal ridges and more granulated ventral skin, and from *G. minima* by larger body and much well developed toe webbing. Diploid chromosomes are homomorphic, i.e., not sexually dimorphic unlike most of *G. rugosa*.

Description of holotype (in millimeters). Snout-vent length (SVL) 40.7; body robust; head large, slightly wider (HW 17.3, 42.5%SVL) than long (HL 16.6, 40.7%SVL); snout triangular, tip slightly pointed in dorsal outline; projecting beyond lower jaw, slightly rounded in lateral profile; canthus very distinct; lore vertical, concave; nostril below canthus, midway between tip of snout (S-NL 3.8, 9.3%SVL) and anterior margin of upper eyelid; internarial distance (IND 3.4, 8.2%SVL) shorter than distance from nostril to eye (N-EL 3.8, 9.4%SVL); eye large, length (EL 5.4, 13.3%SVL) one and half times eye-nostril distance but smaller than snout length (SL 6.9, 17.0%SVL); interorbital (IOD 3.9, 9.5%SVL) subequal to width of upper eyelid (UEW 3.9, 9.6%SVL) and wider than internarial distance; pineal spot present; tympanum large and very distinct, nearly circular (TD 4.7, 11.6%SVL), about five-sixth eye diameter; vomerine teeth in indistinctly oval, small, and slightly oblique raised series (each of 2 teeth), the center posterior to line connecting posterior margins of choanae, narrowly separated from each other, but widely separated from choanae; tongue narrow anteriorly, moderately notched, without papilla; a pair of internal vocal sacs and vocal openings on corners of mouth.

Forelimb stout (FLL 26.9, 66.1%SVL; LAL 20.4, 50.0%SVL; FAW 3.9, 9.6%SVL); fingers slender unwebbed, but with fringes of skin; finger length formula: II<I<IV<III (Fig. 6C), first finger as long as second; finger tips blunt, without disk; three large palmar tubercles, and indistinct supernumerary tubercles; subarticular tubercles prominent, circular; distinct gray nuptial pads on dorsal, medial, and ventral surfaces of first finger extending from its base to distal phalanx, covered with minute asperities.

Hindlimb long (HLL 71.4, 175.4%SVL), about 2.6 times the length of forelimb; tibia (TL 21.5, 52.8%SVL) shorter than foot (FL 23.7, 58.3%SVL); heels overlapping when limbs are held at right angles to body; tibiotarsal articulation of adpressed limb reaching anterior corner of eye; toe tips blunt, without disk; toe length formula I<II<III<V<IV; third toe shorter than fifth; toes moderately webbed, formula I 1/2–$1^1/_2$ II 1–2 III 1/2–2 IV $1^1/_2$–0 V (Fig. 6D); excision of membrane between two outer toes reaching the point between distal and middle subarticular tubercles of fourth when toes in contact; webs thick, not crenulate; subarticular tubercles prominent, rounded; inner metatarsal tubercle distinct, oblong (IMTL 2.1, 5.2%SVL), less than half length of first toe (5.0, 12.2%SVL); outer metatarsal tubercle small but distinct; tarsus with strong tarsal fold.
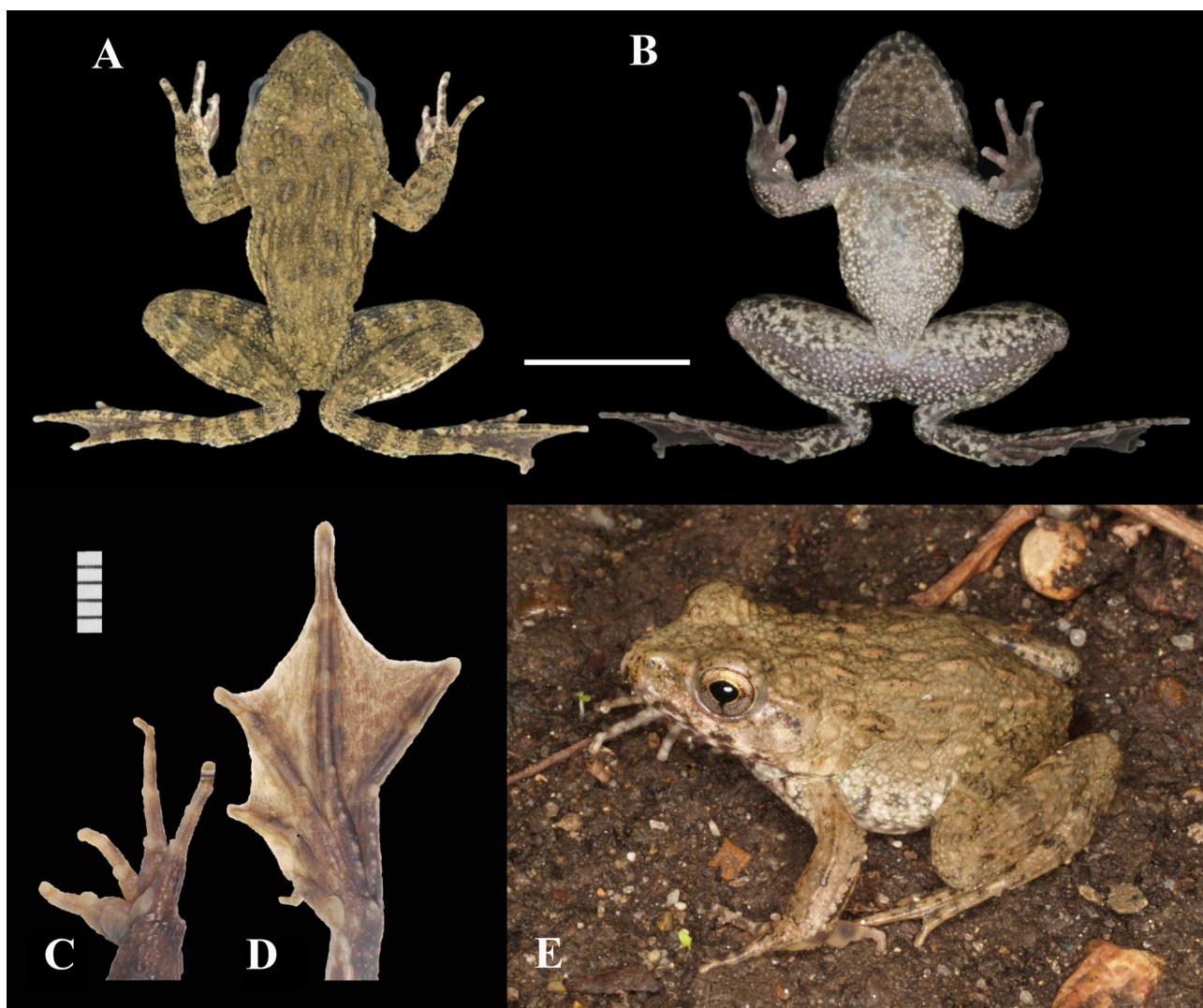

FIGURE 6. Dorsal (A) and ventral (B) views of the whole body and ventral view of left hand (C) and foot (D) of the male holotype of *Glandirana reliquia* **sp. nov.** (KUHE 64088). Scale bar = 20 mm (A, B)/5 mm (C, D). A lateral view of a nearly topotypic male in life (AUEZ 0843: Kamogawa City, Chiba Prefecture) is shown as well (E).

Head dorsally covered with small tubercles. Dorsum from posterior to upper eyelid to anterior to vent, covered with longitudinal skin folds, with pustular warts and granules in between; no dorsolateral fold; a supratympanic fold from eye, but not curved to axilla; side of trunk coarsely granular; longitudinal skin folds dorsally on forearm and tibia; ventral side weakly rugose.

Color in life. Dorsum dark brown with faint dark blotches, but without interorbital bar; no vertebral line medially;

lores with light dark markings below canthus; upper lip with dark bars; upper half of tympanum surrounded by a weak brown band; limbs marked dorsally with dark brown crossbars; ventrum light brown scattered with minute white spots; blackish brown bar on lower lip not clear; ventral surfaces of thigh and tibia with irregular dark spots.

Variation. A summary of morphometric data is shown in Table 2 together with those on mitochondrial groups of *G. rugosa*. Females are significantly larger in SVL (mean ± SD = 47.9 ± 1.4 mm, n = 35) than males (36.8 ± 1.0 mm, n = 41; t-test, P < 0.01). Size of all characters relative to SVL, except for FFL, tended to be greater in males than females (Mann-Whitney U-test, two-tailed, P < 0.05). When the hindlimb was bent forward along the body, tibiotarsal joint reached the point between middle of upper eyelid and nostril in males, and between posterior and anterior corners of upper eyelid in females, but the medians had no sexual difference, both to the point anterior to upper eyelid. Males tended to have more developed toe webbing than females, and the incision of outer web in males varied from distal to same level of middle subarticular tubercles on fourth toe, with the median same level of middle subarticular tubercles. In contrast, females had the incision from same level to proximal to middle subarticular tubercles on fourth toe, with the median proximal to middle tubercles.

Degree of development of larval ventral glands varied among populations, and medians ranged from state B (Kimitsu, 41.7%; Sendai, 33.3%) through state C (Hiratsuka, 16.7%) to state D (Higashichichibu, 72.7%), with the ground median state C (see below).

Eggs and larvae. In a population from Matsudo City, Chiba Prefecture, eggs laid at a time ranged from 892–1452 (mean ± SD = 1245 ± 246, n = 4) (Okada 1930). In the paratypic female, left ovary contained 627 mature eggs, each 1.3 mm in diameter and light brown in animal hemisphere. Eggs are laid in small clumps of about 30 to 60 eggs.

A total of nine overwintered tadpoles in stages 31–35 (total length [TOTL] = 37.8–53.6 [mean ± SD = 45.2 ± 14.5] mm, head body length [HBL] = 13.0–20.3 [mean ± SD = 16.4 ± 1.6] mm), and two in stages 36–41 (TOTL = 46.9–55.9 [mean = 51.4] mm, HBL=18.1–18.6 [mean = 18.3] mm), from the type locality were closely examined. Head and body slightly flattened above, spheroidal below; head body width (HBW) maximum slightly anterior to level of spiracle 59–69% (median = 63%) of HBL; head body depth (HBD) 74–90% (median = 83%) of HBW; snout rounded; eyes dorsolateral, not visible from below; nostril open, dorsolateral, rim raised, midway between tip of snout and eye; internarial 100–101% (median = 101%) of interorbital. Oral disk anteroventral, emarginate, width 33–34% (median = 33%) of HBW; marginal papillae on upper labium with wide gap; lower labium with a continuous row of papillae, submarginal papillae present near corners; denticles 2(2)/3(1) (Fig. 7D); beaks with black outer margins; outer surface smooth; margin finely serrate; upper beak weekly convex medially; neither beak divided. Spiracle sinistral, tube pointing upward and backward, free of body wall slightly. Anal tube dextral, attached to ventral fin; loops of gut visible ventrally only in young larvae. Tail moderately long and lanceolate, both margins weakly convex, tapering gradually to slightly rounded tip; tail length 164–199% (median = 175%) of HBL, maximum depth 26–44% (median = 31%) of length; dorsal fin origin at posterior end of body, deeper than ventral fin except near tail tip; ventral fin origin continuous to vent; caudal muscle moderately strong, maximum tail width 26–40% (median = 31%) of HBW; muscle depth at anterior one-third of tail 45–59% (median = 50%) of tail depth, steadily narrowed posteriorly, shallower than either fin in distal half of tail. Indistinct supranaso-orbital, infranaso-orbital, mental, pregular, and lateral neuromasts discernible. Larval skin glands variously developed but overall very few on dorsum (Yamamoto & Shimada 2021). Ventral glands also variable, but the median was state C (glands partly absent between throat and abdomen, center of abdomen without glands). In life dorsal and lateral body brown, spotted with black and covered with silver; venter dirty white, scattered with dark gray on throat; tail scattered with black and densely covered by silver spots (Fig. 7A–C).

Karyotype. Diploid chromosome 2n = 26, with five large and eight small pairs, that are homomorphic and lacking sexual difference (Nishioka *et al.*, 1994). Chromosome Nos. 1, 2, 4, and 5 in the larger group and Nos. 6, 8 and 10 in the smaller group are metacentric, while Nos. 3 in the larger group and Nos. 9, 11, 12, and 13 in the smaller group are submetacentric. The small chromosome No. 7 is subtelocentric, of which short arm is shorter than that of subtelocentric chromosome 7 in *G, rugosa* (Miura *et al.*, 1998; Ogata *et al.*, 2002). The small chromosome No. 11 has a distinct secondary constriction in the longer arm.

Call. We analyzed mating calls of a single male, recorded at a paddy field at Osho, Itsukaichi, Akiruno City, Tokyo at an air temperature of 20.1°C on 4 June 2013 by N. Maeda. Calls (15 notes were analyzed) consisted of a series of notes each emitted at an interval (between the beginnings of two successive notes) of 0.56 ± 0.08 (0.48–0.77) s (Fig. 8). Each note was composed of 22.4 ± 6.2 (17–37) short pulses and lasted for 0.39 ± 0.12 (0.29–0.65) s. Frequency bands spread over the 0.56–2.5 kHz range, and the dominant frequency was 0.84 ± 0.04 (0.76–0.91) kHz. Frequency and intensity modulations were only slight.

Comparisons. The new species tends to be different from the groups of *G. rugosa* in much less developed larval dorsal skin glands (Yamamoto & Shimada 2021). Compared with the Central group of *G. rugosa*, *G. reliquia* **sp. nov.** differs by relatively longer limbs (forelimb, lower arm, outer palmar tubercle, hand, hindlimb, tibia, and foot) in both sexes. Also, the new species has wider upper eyelid margin and longer first toe in females, and third finger in males, but has smaller inner metatarsal tubercle in females. From the North group of *G. rugosa*, the new species is distinguished by having relatively wider upper eyelid margins and longer limbs (forelimb, lower limb, outer palmar tubercle, hand, foot, and first toe) in both sexes, and in third finger length in males. Compared with the Western group of *G. rugosa*, the new species has relatively longer limb parts (forelimb, hindlimb, tibia, and foot) in both sexes, and in longer snout-nostril and larger tympanum in females.
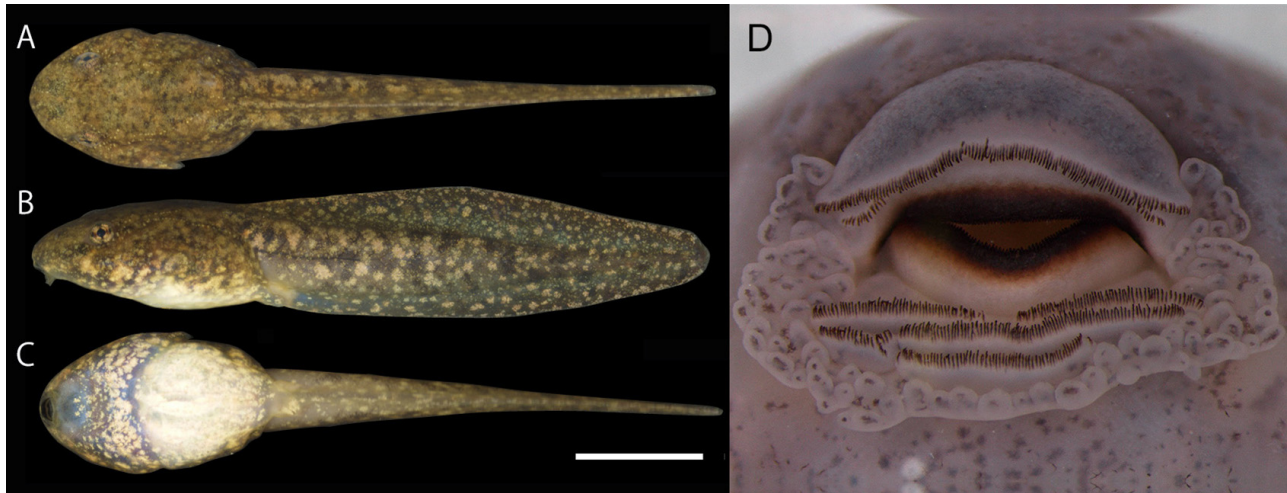
FIGURE 7. Dorsal (A), lateral (B), and ventral (C) views and the oral disc (D) of a tadpole of *Glandirana reliquia* **sp. nov.** in stage 35 of Gosner (1960), collected on 9 May 2013 at Sendai City, Miyagi Pref., Japan. Scale bar = 10 mm.
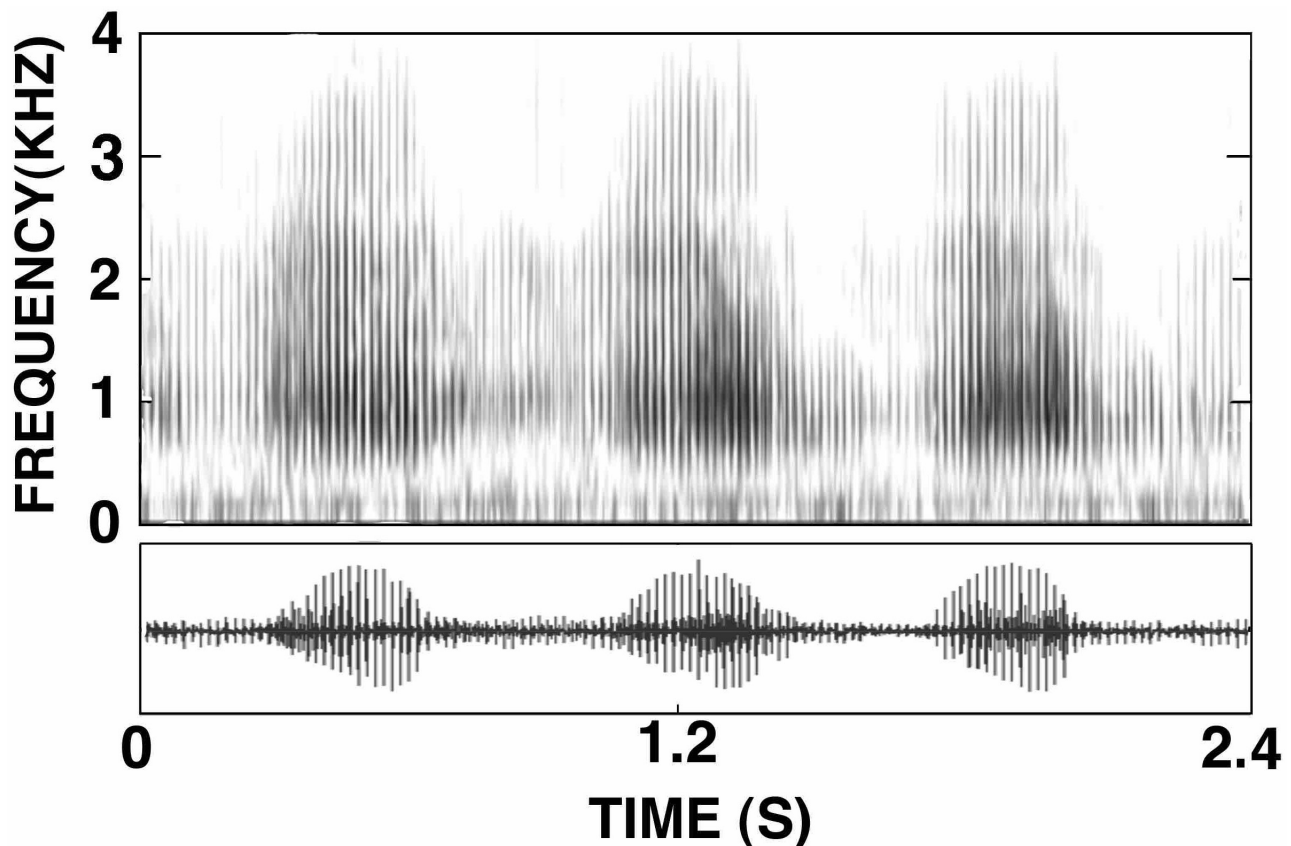

FIGURE 8. Advertisement call of *Glandirana reliquia* **sp. nov.** from Tokyo, Japan, recorded at an air temperature of 20.1°C, showing sonogram (top) and wave form (bottom).

From *G. susurra*, *G. reliquia* **sp. nov.** is distinct in having relatively longer (head, snout, tympanum) and wider head parts (head width, upper eyelid, upper eyelid margin), and longer finger (third finger and first finger) in both sexes, and larger nostril-eye, intercanthal, and hand, and smaller inner palmar tubercle in females. Compared with *G. emeljanovi*, the new species has relatively larger head parts (tympanum, head width, upper eyelid margin) and limbs (forelimb, lower arm, third finger, first finger, hand, hindlimb, and foot) in both sexes, and larger eye, upper eyelid, and first toe in females.

Of the two remaining members of wrinkled frogs, *G. tientaiensis* (Chang 1933) resembles *G. reliquia* **sp. nov.**, but has much flatter dorsal ridges and less granulated ventral skin than the latter. *Glandirana minima* (Ting & Tsai 1979) has significantly smaller body and much less developed toe webbing than *G. reliquia* **sp. nov.** (Fei *et al.* 2012).

Range. Eastern half of southern Tohoku to Kanto and Chubu regions (Fig. 9). Eastern Tohoku region: Iwate Prefecture (Oshu City, Kitakami City, Ichinoseki City [former Higashiyama Town], Hiraizumi Town, Tono City, Hanamaki City), Miyagi Prefecture (Minamisanriku Town, Sendai City, Kawasaki Town), Fukushima Prefecture (Iwaki City). Kanto region: Ibaraki Prefecture (Tsukuba City, Hitachiomiya City), Tochigi Prefecture (Ichikai Town, Ashikaga City, Nasushiobara City, Utsunomiya City, Kanuma City), Gunma Prefecture (Shibukawa City [former Akagi Village], Katashina Village), Saitama Prefecture (Ogawa Town, Higashichichibu Village), Chiba Prefecture (Mobara City, Kamogawa City, Kimitsu City, Ichihara City), Tokyo Metropolis (Akiruno City [former Itsukaichi Town]), Kanagawa Prefecture (Yamakita Town, Odawara City, Sagamihara City, Minamiashigara City, Isehara City). Chubu region: Yamanashi Prefecture (Kofu City, Uenohara City), Nagano Prefecture (Nakano City, Yamanouchi Town, Nagano City [former Togakushi Village], Chikuma City, Ueda City, Tomi City, Komoro City, Saku City, Matsumoto City, Shiojiri City, Hakuba Village, Minamimaki Village).

Natural History. *Glandirana reliquia* **sp. nov.** inhabits widely plains and low mountains, near various water bodies from artificial ponds in urban area to paddy fields, rivers, montane streams, and wetlands. Breeds during late May and late August in still waters in rice fields, ponds, ditches, sometimes in pools of dry riverbeds, but also in slowly flowing waters. Multiple clutches spawned by some females in a year.

Eggs are laid in small batches on vegetations in the shallow water of very slowly flowing interceptor connecting water canals and paddies. Ashizawa *et al.* (2013) reported flow velocity to have the most impact on the egg batch density, in Ichikai Town, Tochigi Prefecture. Larvae hatched from eggs laid at the end of breeding season usually overwinter and metamorphose in the following year.

Conservation status. *Glandirana rugosa* including *G. reliquia* **sp. nov.** is listed as Least Concern (LC) in IUCN category (Matsui *et al.* 2021). It is not listed in Japanese Red List by Ministry of Environment, but populations assigned to *G. reliquia* **sp. nov.** is variously treated to levels of Critically Endangered (Chiba Prefecture), Endangered (Saitama Prefecture), Vulnerable (Tochigi, Gunma, and Nagano Prefectures and Tokyo Metropolis), and near threatened (Miyagi Prefecture) by local governments in the range of its distribution.

Discussion

Taxonomic status of genetic groups found in *G. rugosa*. We could confirm paraphyly of *G. rugosa* in the mtDNA phylogeny with respect to related species as reported by previous authors (Sekiya *et al.* 2012; Oike *et al.* 2017). Uncorrected p-distances in 16S rRNA observed among groups of *G. rugosa*, and *G. susurra* (3.1–7.0%: Table 1) are large compared with other Japanese frogs (e. g. *Odorrana narina* (Stejneger) vs. *O. amamiensis* (Matsui): 2.6%; *O. ishikawae* (Stejneger) vs. *O. splendida* Kuramoto, Satou, Oumi, Kurabayashi, et Sumida: 1.6%; Matsui *et al.* 2005). Thus, overall high genetic diversity suggests the presence of cryptic species within *G. rugosa*, and a taxonomic revision was therefore required for this species.

However, in the SNP analyses representative of the nuclear genome, only the East group (*G. reliquia* **sp. nov.**) was clearly separated from the remaining *G. rugosa*. Thereby, evolutionary history of *G. rugosa* estimated from nuclear genome greatly differed from that estimated from mtDNA genome. The reason for this discrepancy will be discussed later, but may partly be derived from the properties of mtDNA, such as maternal inheritance, and often affected by gene penetration. In any case, we consider the results of SNP analyses that stand on total genome information to be more correctly reflecting evolutionary history of populations than results obtained from mtDNA.
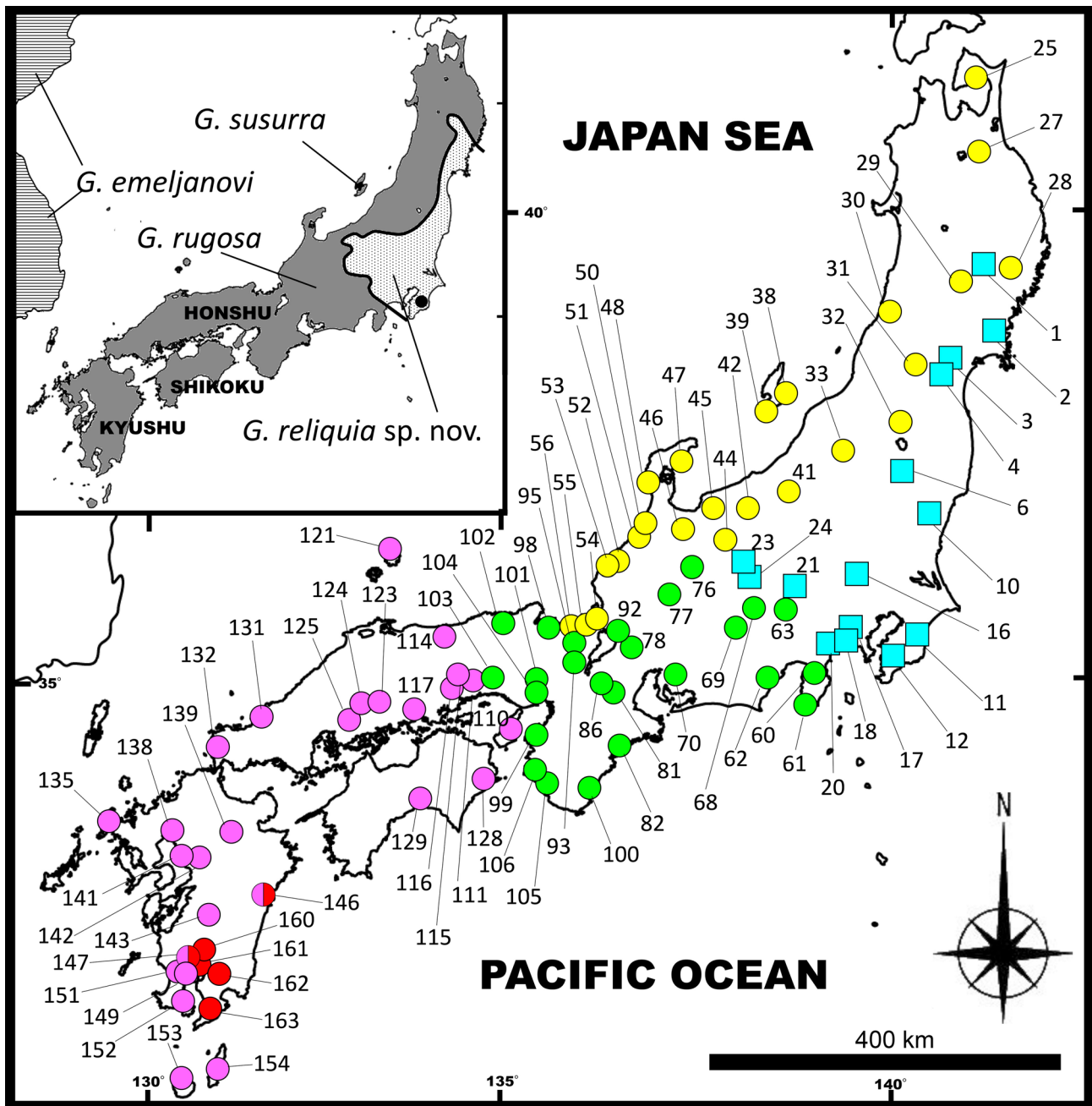
FIGURE 9. Map of Japan showing our results and the conclusion. Upper left: distributional ranges of *Glandirana reliquia* **sp. nov.** (dotted area, closed circle = type locality) and *G. rugosa* (gray area). Lower right: the sites where we collected molecular samples of *Glandirana reliquia* **sp. nov.** (squares) and four mtDNA groups of *G. rugosa* (circles). Locality numbers correspond with those shown in the supplementary Table 1 deposited in Figshare (DOI: 10.6084/m9.figshare.20290599) .

Between *G. reliquia* **sp. nov.** (East group) and the neighboring groups (North and Central), no trace of past hybridization could be detected from SNP analysis, even between very closely situated localities. For example, each of geographic distance between Matsumoto City (East) and Omachi City (North), between Shiojiri City (East) and Ina City (Central), and between Minamiashigara City (East) and Kannami Town (Central) is only about 30 km. Among these cases, the last one might be isolated by the Hakone Mountain Range, but in the former two, no clear geographic barrier exists between them. However, each combination of populations can be very clearly differentiated based on their nuclear genome. These lines of evidence indicate the presence of isolation between *G. reliquia* **sp. nov.** (East group) and other groups of *G. rugosa,* corresponding to specific level isolation. Nevertheless, we failed to morphologically distinguish adult *G. reliquia* **sp. nov.** (East group) from the others as in the previous studies (Sekiya *et al.* 2012; Shimada 2015; Oike *et al.* 2020).

Even so, distinctness of *G. reliquia* **sp. nov.** is clear from the molecular genetic analyses presented herein. We could not find diagnostic morphological characteristics in adults, but found significantly less developed ventral glands in larval *G. reliquia* **sp. nov.** This result concorded with a preliminary study of Yamamoto & Shimada (2019), who reported much more scarce dorsal skin glands than the other groups in the larvae of the East group. Regarding acoustic characteristics, important for anurans as a premating isolating mechanism, marked differences have never been reported between *G. reliquia* **sp. nov.** (East group) and Central groups, but *G. reliquia* **sp. nov.** (East group) is reported to have differences from the North group in call length and pulse number (Hasegawa *et al.* 1999). It is necessary in the future to study various characters like this for further clarifying groups of *G. rugosa* that so far we left unchanged taxonomically.

Evolutionary history of *Glandirana* within Japan. Molecular analyses resulted in quite different results between mtDNA and SNPs. A close relationship in mtDNA of *G. reliquia* **sp. nov.** (East group) and Central group of *G.* (as *Rana*) *rugosa* has been supported by previous analyses of allozymes (Nishioka *et al.* 1993), but was completely denied by our analyses of SNPs. This discrepancy is enigmatic because allozymic analysis is based on nuclear information, and thus would be expected to recover similar relationships as the SNPs, compared with mtDNA.

However, in the locus examined in the allozymic study of Nishioka *et al.* (1993), we can see various types of geographic pattern. For example, in IDH-B (isocitrate dehydrogenase), similarity between East and Central groups agreeing with mtDNA analysis was supported, but in LDH-B (lactate dehydrogenase), apparent similarity between East and North groups was detected. On the other hand, in AK (adenylate kinase) and Hb-II (hemoglobin), East group exhibited unique genetic features. Although Nishioka *et al.* (1993) examined 25 loci, some of them contained only subtle allelic variations, and the dendrogram might be seriously affected by the certain loci with enough amounts of variation. If such an influential locus accidentally contains the wrong genetic information, the dendrogram would be seriously biased. Compared with allozymic analysis, SNP analyses stand on much more fine-scale genetic information of nuclear genome, and we thus regard the result of our SNP analyses to reflect the true evolutionary history.

From a mtDNA phylogeny and differentiation pattern in sex chromosomes, Ogata *et al.* (2003) hypothesized that two populations, Kanto type (= East group, *G. reliquia* **sp. nov.**) and West Japan type (= West group), were distributed in east and west, respectively, of Japan, as the ancestral populations of Japanese *G. rugosa*. These two ancestral populations were hypothesized to have hybridized at central Honshu and gave birth to ZW type (= North group) at Hokuriku District and XY type (= Central group) at Tokai District, and at Kinki District, so-called neo-ZW type (= West-Central group) arose through further hybridization of XY type with West Japan type (Ogata *et al.* 2007). However, as far as our results indicate, hybridization of ancestral *G. reliquia* **sp. nov.** (East group) and West group does not seem to be so large as to mingle the whole genome, and the genetic contents of the hybrid populations (North and Central groups) were mostly provided from the ancestral West group. Such hybrid populations are thought to lose genetic contact with *G. reliquia* **sp. nov.** subsequently, but some genetic features such as several allozymes (Nishioka *et al.*, 1993), mtDNA (Sekiya *et al.*, 2010), and chromosome 7 (a prototype of the X chromosome) (Miura *et al.* 1998; Ogata *et al.* 2003; Mawaribuchi *et al.* 2016) are thought to be remained in the Central group. Seemingly close relationships of *G. reliquia* **sp. nov.** (East group) and the Central group in allozymes and mtDNA phylogenies would be the results of such gene penetrance during earlier hybridization events.

We analyzed nearly sympatric West and Southeastern Kyushu groups of *G. rugosa* from two localities (Nobeoka City in Miyazaki Pref. and Satsumasendai City in Kagoshima Pref.), but all individuals were nearly identical in SNPs (Fig. 3). Thus, it is clear that genetic isolation does not exist between the two groups. What is interesting is why the mitochondrial genotype close to East group occurs in southeastern region of Kyushu (se-Kyushu group). One possibility is that the range of the ancestral population of *G. reliquia* **sp. nov.** (East group) was larger than in the present population, covering Kyushu region. Then, in the decreasing process of the ancestral *G. reliquia* **sp. nov.** (East group) population through the enlargement of the West group, partial hybridization occurred between them, and the population keeping mtDNA of the *G. reliquia* **sp. nov.** (East group) while having properties of West group as a whole genome appeared. If these estimations are correct, the population in southeastern Kyushu is very interesting in that it conveys us genetic information of an ancestral population once lost. However, there is no reason to recognize it as a taxonomically valid population as insisted by Oike *et al.* (2020) and Nakamura *et al.* (2022). If we solely rely on mtDNA phylogeny, the Western group is almost surely true *G. rugosa*, and each group of Northern Central, and se-Kyushu *G. rugosa* should be split as a distinct species. Such a classification, however, is not supported at present by the evidence from nuclear genomes.

Summary

In Japanese wrinkled frog, *G. rugosa* sensu lato, five major genetic groups (East, North, Central, West, and southeast Kyushu) have been reported in mtDNA, and relatively large distances among them (3.1-7.0% in 16S rRNA) have suggested the necessity of taxonomic revisions (Nakamura *et al.* 2022). However, through the fine-scale analyses of nuclear genome (SNPs), we found that reliance on mtDNA has seriously misled the conclusions in previous studies. In our SNP analyses, the East group, which we described as *G. reliquia* **sp. nov.**, was genetically distinct from others, and no evidence of present hybridization with neighboring *G. rugosa* (North and Central) was detected. Judging from karyological studies of *G. rugosa* (Miura *et al.* 1998; Ogata *et al.* 2003; Mawaribuchi *et al.* 2016), the W chromosome of the North group and the X chromosome of the Central group were originally derived from the chromosome 7 of *G. reliquia* **sp. nov.** (East group). Further, *G. reliquia* **sp. nov.** (East group) and Central group of *G. rugosa* were relatively close in mtDNA (3.5% in 16S rRNA), forming a cluster in the phylogenetic tree. However, we concluded that these partial similarities were derived from the past genetic introgression from East group to the ancestors of North and Central groups. In our analyses of SNPs, the borders of North, Central, and West groups were not clear, and no apparent genetic gaps existed between them. At present, we suppose that further taxonomic separations are not needed for these groups, although relatively large genetic variations are detected between some of them (~6.8% in 16S rRNA). The Southeast Kyushu group, which was once described as a distinct species by Nakamura *et al.* (2022), shares similar genetic traits with West group in SNP analyses, and we concluded that their unique mtDNA was penetrated from the ancestor of *G. reliquia* **sp. nov.** (East group) to a part of West group, and remained around this area.

Although many studies have pointed to the risk of using mtDNA as sole indicator for demographic, phylogenetic, and phylogeographic purposes (e.g. Ballard & Whitlock 2004; Hurst & Jiggins 2005), this tool has long been used to detect candidates of cryptic species in the studies of biodiversity (e.g. Fouquet *et al.* 2007). The genetic distance of mtDNA has sometimes been used as a simple threshold to judge the validity of cryptic species, and even recently, some Japanese amphibians have been described practically based solely on mtDNA (e.g. Nakamura *et al.* 2022; Sugawara *et al.* 2022). However, at least in some cases, hybridization and subsequent genetic introgression can take place even at very high levels of mtDNA divergence (Malone & Fontenot 2008), and mtDNA is therefore not fully a reliable tool for this purpose. Our present study could be a good example alerting of this risk.

Acknowledgments

References

Ashizawa, K., Osawa, S. & Katsuno, T. (2013) Spawning site selection of *Rana rugosa* in paddy field at bottomland in hilly area. *Papers on Environmental Information Science*, 27, 33–36.
Ballard, J.W.O. & Whitlock, M.C. (2004) The incomplete natural history of mitochondria. *Molecular Ecology*, 13, 729–744.
    https://doi.org/10.1046/j.1365-294X.2003.02063.x
Bolger, A.M., Lohse, M. & Usadel, B. (2014) Trimmomatic: a flexible trimmer for Illumina sequence data. *Bioinformatics*, 30, 2114–2120.
    https://doi.org/10.1093/bioinformatics/btu170
Castresana, J. (2000) Selection of conserved blocks from multiple alignment for their use in phylogenetic analysis. *Molecular Biology and Evolution*, 17, 540–552.

https://doi.org/10.1093/oxfordjournals.molbev.a026334

Catchen, J., Amores, A., Hohenlohe, P., Cresko, W. & Postlethwait, J. (2011) Stacks: building and genotyping loci de novo from short-read sequences. *G3: Genes, Genomes, Genetics*, 1, 171–182.
https://doi.org/10.1534/g3.111.000240

Chang, T.K. (1933) Two new amphibian records from Chekiang. *Peking Natural History Bulletin*, 8, 75–80.

Dubois, A. (1992) Notes sur la classification des Ranidae (Amphibiens anoures). *Bulletin Mensuel de la Société Linnéenne de Lyon*, 61, 305–352.
https://doi.org/10.3406/linly.1992.11011

Earl, D.A. & von Holdt, B.M. (2012) STRUCTURE HARVESTER: A website and program for visualizing STRUCTURE output and implementing the Evanno method. *Conservation Genetics Resources*, 4, 359–361.
https://doi.org/10.1007/s12686-011-9548-7

Evanno, G., Regnaut, S. & Goudet, J. (2005) Detecting the number of clusters of individuals using the software Structure: a simulation study. *Molecular Ecology*, 14, 2611–262.
https://doi.org/10.1111/j.1365-294X.2005.02553.x

Fei, L., Ye, C.-Y. & Jiang, J.-P. (2010) Phylogenetic systematics of Ranidae. *Herpetologica Sinica*, 12, 1–43.

Fei, L., Ye, C.-Y. & Jiang, J.-P. (2012) *Colored Atlas of Chinese Amphibians and Their Distributions*. Sichuan Publishing House of Science & Technology, Sichuan.

Fouquet, A., Gilles, A., Vences, M., Marty, C., Blanc, M., & Gemmell, N.J. (2007) Underestimation of species richness in Neotropical frogs revealed by mtDNA analyses. *PLoS ONE*, 2 (10), e1109.
https://doi.org/10.1371/journal.pone.0001109

Frost, D.R., Grant, T., Faivovich, J.N., Bain, R.H., Haas, A., Haddad, C.F.B., de Sá, R.O., Channing, A., Wilkinson, M., Donnellan, S.C., Raxworthy, C.J., Campbell, J.A., Blotto, B.L., Moler, P., Drewes, R.C., Nussbaum, R.A., Lynch, J.D., Green, D.M. & Wheeler, W.C. (2006) The amphibian tree of life. *Bulletin of the American Museum of Natural History*, 297, 1–370.
https://doi.org/10.1206/0003-0090(2006)297[0001:TATOL]2.0.CO;2

Gasso Miracle, M.E., van den Hoek Ostende, L.W. & Arntzen, J.W. (2007) Type specimens of amphibians in the National Museum of Natural History, Leiden, The Netherlands. *Zootaxa*, 1482 (1), 25–68.
https://doi.org/10.11646/zootaxa.1482.1.2

Gosner, K. (1960) A simplified table for staging anuran embryos and larvae with notes on identification. *Herpetologica*, 16, 183–190.

Hasegawa, Y., Ueda, H. & Sumida, M. (1999) Clinal geographic variation in the advertisement call of the wrinkled frog, *Rana rugosa*. *Herpetologica*, 55, 318–324

Hillis, D.M. & Bull, J.J. (1993) An empirical test of bootstrapping as a method for assessing confidence in phylogenetic analysis. *Systematic Biology*, 42, 182–192.
https://doi.org/10.1093/sysbio/42.2.182

Huelsenbeck, J.P. & Ronquist, F. (2001) MRBAYES: Bayesian inference of phylogenetic trees. *Bioinformatics*, 17, 754–755.
https://doi.org/10.1093/bioinformatics/17.8.754

Hurst, G.D.D. & Jiggins, F.M. (2005) Problems with mitochondrial DNA as a marker in population, phylogeographic and phylogenetic studies: the effects of inherited symbionts. *Proceedings of the Royal Society B*, 272, 1525–1534.
https://doi.org/10.1098/rspb.2005.3056

Jombart, T. (2008) adegenet: a R package for the multivariate analysis of genetic markers. *Bioinformatics*, 24, 1403–1405.
https://doi.org/10.1093/bioinformatics/btn129

Kozlov, A.M., Darriba, D., Flouri, T., Morel, B. & Stamatakis, A. (2019) RAxML-NG: a fast, scalable and user-friendly tool for maximum likelihood phylogenetic inference. *Bioinformatics*, 35, 4453–4455.
https://doi.org/10.1093/bioinformatics/btz305

Leaché, A.D. & Reeder, T.W. (2002) Molecular systematics of the eastern fence lizard (*Sceloporus undulatus*): a comparison of parsimony, likelihood, and Bayesian approaches. *Systematic Biology*, 51, 44–68.
https://doi.org/10.1080/106351502753475871

Leaché, A.D., Banbury, B.L., Felsenstein, J., Nieto-Montes de Oca, A., & Stamatakis, A. (2015) Short tree, long tree, right tree, wrong tree: new acquisition bias corrections for inferring SNP phylogenies. *Systematic Biology*, 64, 1032–1047.
https://doi.org/10.1093/sysbio/syv053

Maeda, N. & Matsui, M. (1989) *Frogs and Toads of Japan*. Bun-ichi Sogo Shuppan, Tokyo.

Malone, J.H. & Fontenot, B.E. (2008) Patterns of reproductive isolation in toads. *PLoS ONE*, 2 (10), e1109
https://doi.org/10.1371/journal.pone.0003900

Matsui, M. (1984) Morphometric variation analyses and revision of the Japanese toads (Genus *Bufo*, Bufonidae). *Contributions from the Biological Laboratory, Kyoto University*, 26, 209–428.

Matsui, M. (1997) Call characteristics of Malaysian *Leptolalax* with a description of two new species (Anura: Pelobatidae). *Copeia*, 1997, 158–165.
https://doi.org/10.2307/1447851

Matsui, M. & Maeda, N. (2018) *Encyclopedia of Japanese Frogs*. Bun-ichi Sogo Shuppan, Tokyo, 271 pp.

Matsui, M., Shimada, T. & Miura, I. (2021) *Glandirana rugosa*. The IUCN Red List of Threatened Species 2021:

e.T58706A118983374.
https://dx.doi.org/10.2305/IUCN.UK.2021-1.RLTS.T58706A118983374.en

Matsui, M., Okawa, H., Nishikawa, K., Aoki, G., Eto, K., Yoshikawa, N., Tanabe, S., Misawa, Y. & Tominaga, A. (2019) Systematics of the widely distributed Japanese clouded salamander, *Hynobius nebulosus* (Amphibia: Caudata: Hynobiidae), and its closest relatives. *Current Herpetology*, 38, 32–90.
https://doi.org/10.5358/hsj.38.32

Matsui, M., Shimada, T., Ota, H. & Tanaka-Ueno, T. (2005) Multiple invasions of the Ryukyu Archipelago by Oriental frogs of the subgenus *Odorrana* with phylogenetic reassessment of the related subgenera of the genus *Rana*. *Molecular Phylogenetics and Evolution*, 37, 733–742.
https://doi.org/10.1016/j.ympev.2005.04.030

Mawaribuchi, S., Ito, M., Ogata, M., Oota, H., Katsumura, T., Takamatsu, N. & Miura, I. (2016) Meiotic recombination counteracts male-biased mutation (male-driven evolution). *Proceedings of the Royal Society B: Biological Sciences*, 283, 20152691.
https://doi.org/10.1098/rspb.2015.2691

Miura, I. (2007) An evolutionary witness: the frog *Rana rugosa* underwent change of heterogametic sex from XY male to ZW female. *Sexual Development*, 1, 323–331.
https://doi.org/10.1159/000111764

Miura, I., Ohtani, H., Nakamura, M., Ichikawa, Y. & Saitoh, K. (1998) The origin and differentiation of the heteromorphic sex chromosomes Z, W, X and Y of the frog *Rana rugosa*, inferred from the sequences of a sex-linked gene, ADP/ATP translocase. *Molecular Biology and Evolution*, 15, 1612–1619.
https://doi.org/10.1093/oxfordjournals.molbev.a025889

Nakamura, K. & Uéno, S. (1963) *Japanese Reptiles and Amphibians in Colour*. Hoikusha, Osaka.

Nakamura, M., Nakamura, Y., Oike, A., Tojo, K., Suzuki, T. & Ito, E. (2022) A new frog species of the genus *Glandirana* from Southeastern Kyushu, Japan (Anura Ranidae). *EC Veterinary Science*, 7.1, 11–23.

Nishioka, M., Hanada, H., Miura, I. & Ryuzaki, M. (1994) Four kinds of sex chromosomes in *Rana rugosa*. *Scientific Report of the Laboratory for Amphibian Biology, Hiroshima University*, 13, 1–34.

Nishioka, M., Kodama, Y., Sumida, M. & Ryuzaki, M. (1993) Systematic evolution of 40 populations of *Rana rugosa* distributed in Japan elucidated by electrophoresis. S*cientific Report of the Laboratory for Amphibian Biology, Hiroshima University*, 12, 83–132.

Ogata, M., Hasegawa, Y., Ohtani, H., Mineyama, M. & Miura, I. (2008) The ZZ/ZW sex-determining mechanism originated twice and independently during evolution of the frog, *Rana rugosa*. *Heredity*, 100, 92–99.
https://doi.org/10.1038/sj.hdy.6801068

Ogata, M., Lee, J.Y., Kim, S., Ohtani, H., Sekiya, K,, Igarashi, T,, Hasegawa, Y., Ichikawa, Y, & Miura, I. (2002). The prototype of sex chromosomes found in Korean populations of *Rana rugosa*. *Cytogenetic and Genome Research*, 99, 185–193.
https://doi.org/10.1159/000071592

Ogata, M., Ohtani, H., Igarashi, T., Hasegawa, Y., Ichikawa, Y. & Miura, I. (2003) Change of the heterogametic sex from male to female in the frog. *Genetics*, 164, 613–620.
https://doi.org/10.1093/genetics/164.2.613

Ogata, M., Suzuki, K., Yuasa, Y. & Miura, I. (2021) Sex chromosome evolution from a heteromorphic to a homomorphic system by inter-population hybridization in a frog. *Philosophical Transactions of the Royal Society B*, 376, 20200105.
https://doi.org/10.1098/rstb.2020.0105

Oike, A., Watanabe, K., Min, M.-S., Tojo, K., Kumagai, M., Kimoto, Y., Yamashiro, T., Matsuo, T., Kodama, M., Nakamura, Y., Notsu, M., Tochimoto, T., Fujita, H., Ota, M., Ito, E., Yasumasu, S. & Nakamura, M. (2017) Origin of sex chromosomes in six groups of *Rana rugosa* frogs inferred from a sexlinked DNA marker. *Journal of Experimental Zoology*, 327A, 444–452.
https://doi.org/10.1002/jez.2130

Oike, A., Mochizuki, M., Tojo, K., Matsuo, T., Nakamura, Y., Yasumasu, S., Ito, E., Arai, T. & Nakamura, M. (2020) A phylogenetically distinct group of *Glandirana rugosa* found in Kyushu, Japan. *Zoological Science*, 37, 193–202.
https://doi.org/10.2108/zs190007

Okada, Y. (1930) *A Monograph of the Japanese Tailless Batrachians*. Iwanami-shoten, Tokyo, 215 pp.

Pritchard, J.K., Stephens, M. & Donnelly, P. (2000) Inference of population structure using multilocus genotype data. *Genetics*, 155, 945–959.
https://doi.org/10.1093/genetics/155.2.945

Pyron, R.A. & Wiens, J.J. (2011) A large-scale phylogeny of Amphibia including over 2800 species, and a revised classification of extant frogs, salamanders, and caecilians. *Molecular Phylogenetics and Evolution*, 61, 543–583.
https://doi.org/10.1016/j.ympev.2011.06.012

R Core Team. (2014) *R: a language and environment for statistical computing*. R Foundation for Statistical Computing, Vienna (Austria). Available from: http://www.R-project.org/ (accessed 12 May 2022)

Rice, W.R. (1989) Analyzing tables of statistical tests. *Evolution*, 43, 223–225.
https://doi.org/10.1111/j.1558-5646.1989.tb04220.x

Sekiya, K., Miura, I. & Ogata, M. (2012) A new frog of the genus *Rugosa* from Sado Island, Japan (Anura, Ranidae). *Zootaxa*,

3575, 49–62.
https://doi.org/10.11646/zootaxa.3575.1.3

Sekiya, K., Ohtani, H., Ogata, M. & Miura, I. (2010) Phyletic diversity in the frog *Rana rugosa* (Anura: Ranidae) with special reference to a unique morphotype found from Sado Island, Japan. *Current Herpetology*, 29, 69–78.
https://doi.org/10.3105/018.029.0202

Shimada, T. (2015) A comparison of iris color pattern between *Glandirana susurra* and *G. rugosa* (Amphibia, Anura, Ranidae). *Current Herpetology*, 34, 80–84.
https://doi.org/10.5358/hsj.34.80

Shimada, T. & Matsui, M. (2021) Comments on the article titled "Dr. Siebold and six species of Japanese frogs", published in number 1, volume 2021 of Bulletin of the Herpetological Society of Japan. *Bulletin of the Herpetological Society of Japan*, 2021, 217-224.

Shimada, T., Matsui, M., Yambun, P. & Sudin, A. (2011) A taxonomic study of Whitehead's torrent frog, *Meristogenys whiteheadi*, with descriptions of two new species (Amphibia: Ranidae). *Zoological Journal of the Linnean Society*, 161, 157–183.
https://doi.org/10.1111/j.1096-3642.2010.00641.x

Sokal, R.F. & Rohlf, F.J. (1981) *Biometry, 2nd edition*. W. H. Freeman and Co., San Francisco.

Stamatakis, A. (2014) RAxML version 8: A tool for phylogenetic analysis and post analysis of large phylogenies. *Bioinformatics*, 30, 1312–1313.
https://doi.org/10.1093/bioinformatics/btu033

Stejneger, L. (1907) Herpetology of Japan and adjacent territory. *Bulletin of United States Natural Museum*, 58, 1–577.
https://doi.org/10.5479/si.03629236.58.i

Sugawara, H., Naito, J., Iwata, T. & Nagano, M. (2022) Molecular phylogenetic and morphological problems of the Aki salamander *Hynobius akinesis*: description of two new species from Chugoku, Japan. *Bulletin of the Kanagawa Prefectural Museum (Natural Science)*, (51), 35–46.

Suyama, Y. & Matsuki, Y. (2015) MIG-seq: An effective PCR-based method for genome-wide single-nucleotide polymorphism genotyping using the next-generation sequencing platform. *Scientific Reports*, 5, 16963.
https://doi.org/10.1038/srep16963

Tanabe, A.S. (2011) Kakusan4 and Aminosan: two programs for com- paring nonpartitioned, proportional and separate models for combined molecular phylogenetic analyses of multilocus sequence data. *Molecular Ecology Resources*, 11, 914–921.
https://doi.org/10.1111/j.1755-0998.2011.03021.x

Temminck, C.J. & Schlegel, H. (1838) *Fauna Japonica sive descriptio animalium, quae in itinere per Japonianum, jussu et auspiciis superiorum, qui summum in India Batava Imperium tenent, suscepto, annis 1823–1830 colleget, notis observationibus et adumbrationibus illustratis. Volume 3 (Chelonia, Ophidia, Sauria, Batrachia)*. J. G. Lalau, Leiden.

Ting, H.P. & T'sai, M. (1979) A new species of frog (*Rana minimus*) from Fujian Province. *Acta Zootaxonomica Sinica*, 4, 297–300.

Yamamoto, K. & Shimada, T. (2021) Geographic and seasonal variations on the density of dermal glands in larvae of *Glandirana rugosa* and *G. susurra*. *Bulletin of the Herpetological Society of Japan*, 2021, 96–97.